

We are IntechOpen, the world's leading publisher of Open Access books Built by scientists, for scientists

6,900

Open access books available

185,000

International authors and editors

200M

Downloads

Our authors are among the

154

Countries delivered to

TOP 1%

most cited scientists

12.2%

Contributors from top 500 universities



WEB OF SCIENCE™

Selection of our books indexed in the Book Citation Index
in Web of Science™ Core Collection (BKCI)

Interested in publishing with us?
Contact book.department@intechopen.com

Numbers displayed above are based on latest data collected.
For more information visit www.intechopen.com



SPSLs and Dilute-Nitride Optoelectronic Devices

Y Seyed Jalili

Science Research Campus, Islamic Azad University

Iran

1. Introduction

Currently the main concern in GaAs-based dilute nitride research is the understanding of their material properties. There are many contradictory conclusions specially when it comes to the origin of the luminescence efficiency in these systems. Different ideas have been put forward some more plausible than others. However there is a lack of new ideas to overcome the differences. This chapter will address such issues and then finally we will study SPSL structures as an alternative to the the random alloy quaternary GaInNAs for more efficient growth, design and manufacture of optoelectronic devices based on these alloys.

One of the major issues in current studies of GaInNAs is the metastability of the material. To overcome the rather low solubility of N in GaAs or GaInAs, non-equilibrium growth conditions are required, which can be realized only by molecular-beam epitaxy (MBE) Kitatani et al. (1999); Kondow et al. (1996) or metal-organic vapour phase epitaxy (MOVPE) Ougazaden et al. (1997); Saito et al. (1998). Growing off thermal equilibrium implies a certain degree of metastability. The aim of growing GaInNAs, emitting at the telecommunication wavelengths of 1.3 μm and, also 1.55 μm , is only possible by incorporating nearly 40% In and several per cent of N. These concentrations are at the limits of feasibility in MBE and MOVPE growth on GaAs substrates. The emission wavelength of such GaInNAs layers was strongly blue-shifted when, after the growth of the actual GaInNAs layer, the growth temperature was raised for growing AlGaAs-based top layers (such as distributed Bragg reflectors in vertical-cavity surface-emitting laser (VCSEL) structures or for confinement and guiding in edge emitting laser structures). This led to a number of annealing studies which yield somewhat contradictory results Bhat et al. (1998); Francoeur et al. (1998); Gilet et al. (1999); Kitatani et al. (2000); Klar et al. (2001); Li et al. (2000); Pan et al. (2000); Polimeni et al. (2001); Rao et al. (1998); Spruytte et al. (2001a); v H G Baldassarri et al. (2001); Xin et al. (1999). This, ofcourse, is partly due to the different annealing conditions and growth conditions used, but is also a strong manifestation of the metastability of this alloy system. The full implications of the metastability are just evolving and different mechanisms causing a blue shift of the band gap have been suggested Grenouillet et al. (2002); Mussler et al. (2003); Spruytte et al. (2001b); Tournie et al. (2002); Xin et al. (1999). Nevertheless, all discussions and investigations, so far, have suggested that GaInNAs material system is a very promising candidate for telecoms and in particular datacom applications. However, for both GaNAs and GaInNAs material systems, the higher the nitrogen incorporation, the weaker the alloy luminescence efficiency. A key to the utilization of nitride-arsenide for long wavelength optoelectronic devices is obtaining low defect materials with long non-radiative

lifetimes. Therefore currently, these materials must be annealed to obtain device quality material. Photoluminescence and capacitance-voltage measurements indicate the presence of a trap associated with excess nitrogen Hsu Ho & Stringfellow (1997); Spruytte et al. (2001a). Therefore the likely defect responsible for the low luminescence efficiency is associated with excess nitrogen. It is believed that the effect of thermal annealing on the PL properties of these structures is generally attributed to the elimination of non-radiative centers and improved uniformity. Non-radiative centers are considered to originate from phase separation and/or plasma damage from the N radicals Kitatani et al. (2000).

Interest in the tertiary material system GaNAs had been waned in favour of the quaternary GaInNAs due to its inability to reach the long wavelengths required for commercial applications. However, its new-found use in diffusion-limiting layers and in short-period superlattice structures, and of course being the simpler, ternary, dilute nitride equivalent of GaInNAs and therefore, probably, easier to investigate and understand means that its material properties and behaviour upon annealing are not only important but useful considerations Gupta et al. (2003); Sik et al. (2001). The post-growth rapid thermal annealing (RTA) is usually performed on these ternary Francoeur et al. (1998) and quaternary alloys Spruytte et al. (2001b). Rapid thermal anneal strongly improves the photoluminescence (PL) efficiency. This increase in PL intensity is usually accompanied with a blue shift of the PL peak. In the following section, we focus on the effect of emission energy changes in the photoluminescence (PL) spectrum with annealing of the GaNAs material system and try to elucidate the controversy over its origin.

2. Annealing effects

2.1 Annealing of the ternary GaAs-based dilute nitride: GaNAs

In order to investigate the effect of annealing on this ternary dilute nitride, the sample structure shown in figure 1 was devised. It consists of a 5×8 nm MQW structure, which would provide a good PL signal, and that 8 nm wells (a few nm smaller than the critical thickness for GaNAs layers) would prevent strain relaxation-related defects. Another reason for using an 8 nm well was that a model of emission from a GaNAs MQW structure used to compute emission energies for different well thicknesses and different nitrogen concentrations indicates that. As the well width increases, the nitrogen concentration has increasingly less influence on the bandgap, and so slight growth-rate-related variations in well thickness will have less of an effect on emission.

Samples with nitrogen concentrations of 1.0% and 2.5% were grown for our annealing studies. The lower limit of 1.0% was chosen because it had been suggested theoretically (and has since been demonstrated experimentally) that up to about 1.0%, the coexistence of strongly perturbed host states (PHS) and localized cluster states (CS) of an isoelectronic nitrogen impurity is observed, reflecting the non-amalgamation character of the band formation process Kent & Zunger (2001a;b); Klar et al. (2003). In other words, GaNAs begins to act as a 'dilute nitride' at around $y = 1.0\%$. Samples with 2.5% nitrogen were also grown, as this is approximately the upper limit at which XRD data reflects the total nitrogen content of the sample. It was also thought that if nitrogen out-diffusion was to be responsible for the changes seen as a result of annealing, the sample with higher-nitrogen concentration might, or should, illustrate this more clearly than the sample with lower-nitrogen content.

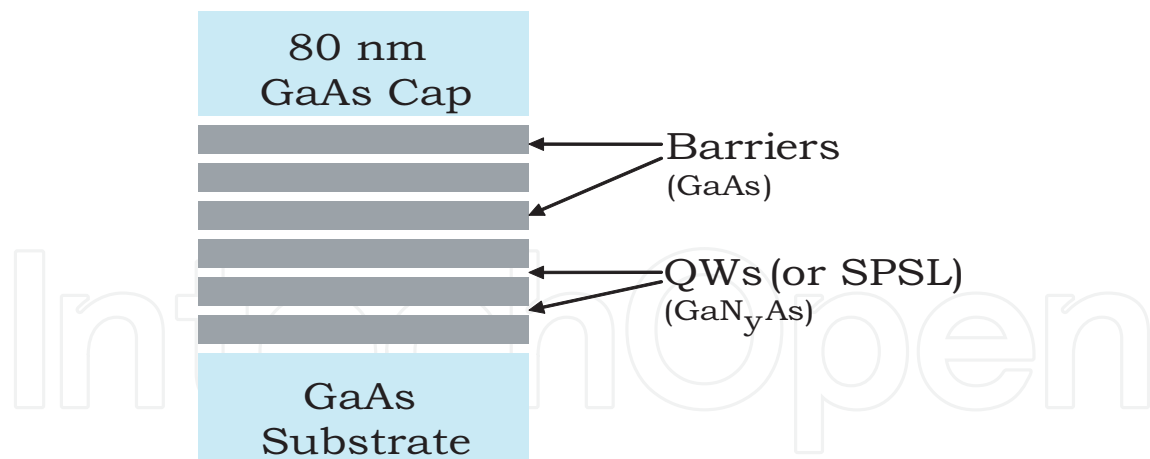


Fig. 1. Schematic nominal GaNAs/GaAs MQW structure used for annealing studies.

Sample Name	Nominal N-Concentration	RTA Round 1	RTA Round 2	Total
GaNAs21	1%	15 sec	30 sec	45 sec
GaNAs22	2.5%	15 sec	30 sec	45 sec
GaNAs23	1%	30 sec	30 sec	60 sec
GaNAs24	2.5%	30 sec	30 sec	60 sec

Table 1. Table showing the RTA times for different samples at 800°C.

PL measurements were made on the as-grown samples at 15 K and also after two ex-situ, RTA treatments, see figures 2 and 3, which were performed at 800°C in ambient Ar using a GaAs (001) insulating substrate proximity cap. Table 1 shows how the first and second rounds of annealing were carried out so that the maximum amount of information could be extracted from only three treatments. In this way, PL could be measured for two different nitrogen concentrations and for five different annealing times, 0 s (as-grown), 15 s, 30 s, 45 s and 60 s. Upon annealing, the peak wavelength of the 1.0% nitrogen samples blue shifted from 1.340 to 1.356 eV (at approx. 0.3 meV s⁻¹), and the full-width half-maximum (FWHM) decreased from 65 to 23 meV (see figures 2). For the 2.5% nitrogen samples, the peak wavelength blue shifted from 1.176 to 1.207 eV (at approx. 0.5 meV s⁻¹), and the FWHM decreased from 38 to 22 meV, see figure 3. Blue shifting, increased peak intensity and decreased FWHM are all effects typical of a post-growth annealing treatment, the changes observed here are in agreement with those reported by Buyanova *et al* Buyanova, Pozina, Hai, Thinh, Bergman, Chen, Xin & Tu (2000) for similar MQW samples and annealing conditions. The fact that the rate of blue shifting for the 2.5% sample is greater than (almost double) that of the 1.0% sample suggests that the underlying mechanism may be N-dependent, but further work would be needed to verify this.

The main changes that occur due to thermal annealing, i.e. a blue shift in peak wavelength and an improvement in integrated intensity and FWHM, have proved rather difficult to explain

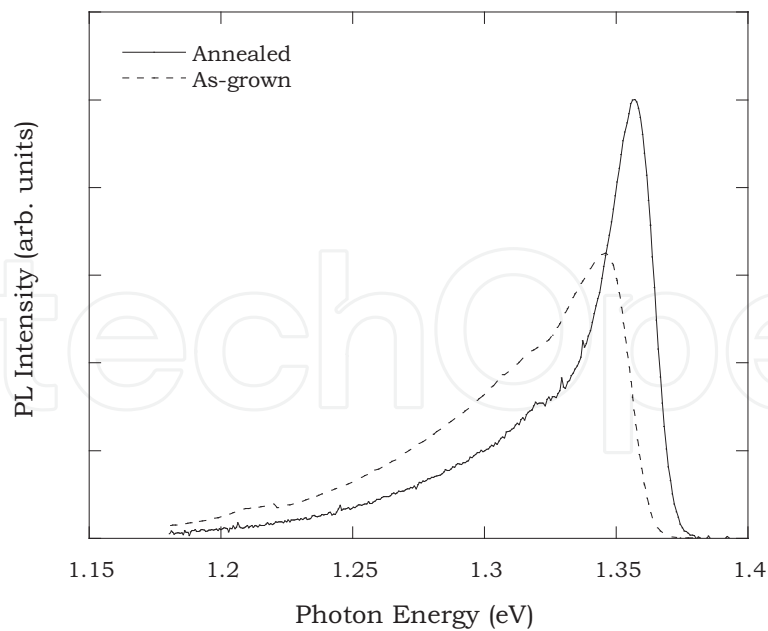


Fig. 2. 15K PL spectra for a five-quantum-well GaN_{0.025}As/GaAs structure grown by SS-MBE and annealed at 800°C for different lengths of time.

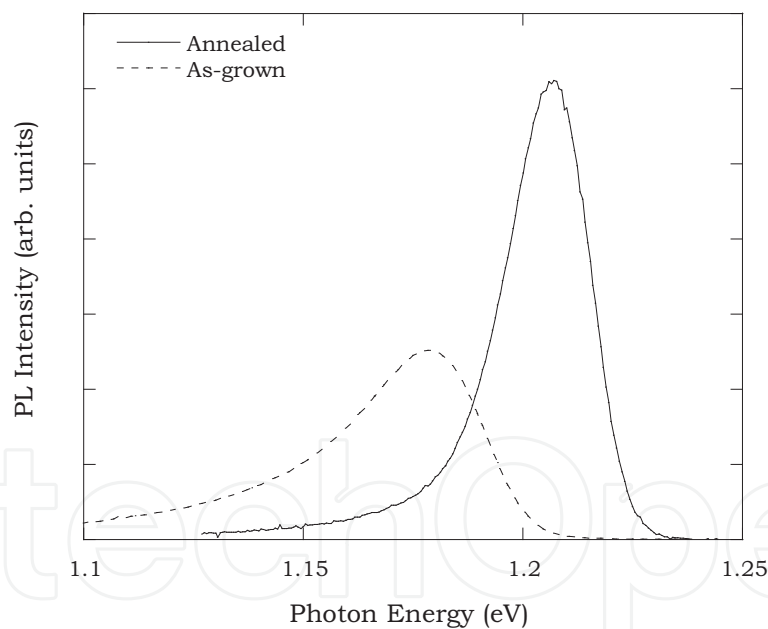


Fig. 3. 15K PL spectra for a five-quantum-well GaN_{0.025}As/GaAs structure grown by SS-MBE and annealed at 800°C for different lengths of time.

in terms of the physical properties of the alloy, and definitive explanations remain elusive, due, as already mentioned, in part to the sometimes contradictory nature of published results Grenouillet et al. (2002); Li, Pessa, Ahlgren & Decker (2001).

Two possible explanations have, so far, been proposed to account for the observed blue shift of GaNAs PL spectra with annealing. Li *et al* Li et al. (2000) observed a RTA-induced blue shift in the low temperature photoluminescence (LTPL) spectrum of a single GaNAs quantum

well and explained it quantitatively by nitrogen diffusion out of the quantum well. On the other hand, Buyanova *et al* Buyanova, Hai, Chen, Xin & Tu (2000) performed low temperature optical studies of both GaNAs multi-quantum wells and thick epilayers and showed that annealing could induce a blue shift of the PL spectra without necessarily changing the photoluminescence excitation (PLE) spectra energy, that is, the peak PL emission wavelength. They therefore suggested that the change in the PL maximum was related to improvement of the alloy uniformity and that RTA decreased the value of the localization potential. This implied that nitrogen preferentially reorganized in the GaNAs layers rather than diffused into the GaAs barriers. Further investigations by Grenouillet *et al* Grenouillet et al. (2002), confirms the explanation by Buyanova *et al*, that nitrogen reorganizes into the narrow band gap GaNAs material rather than escapes out of it. However it is important, ofcourse, to be aware that this peculiar behaviour reflects the interplay of growth conditions, which is a whole research area of its own, as well as metastability in this system.

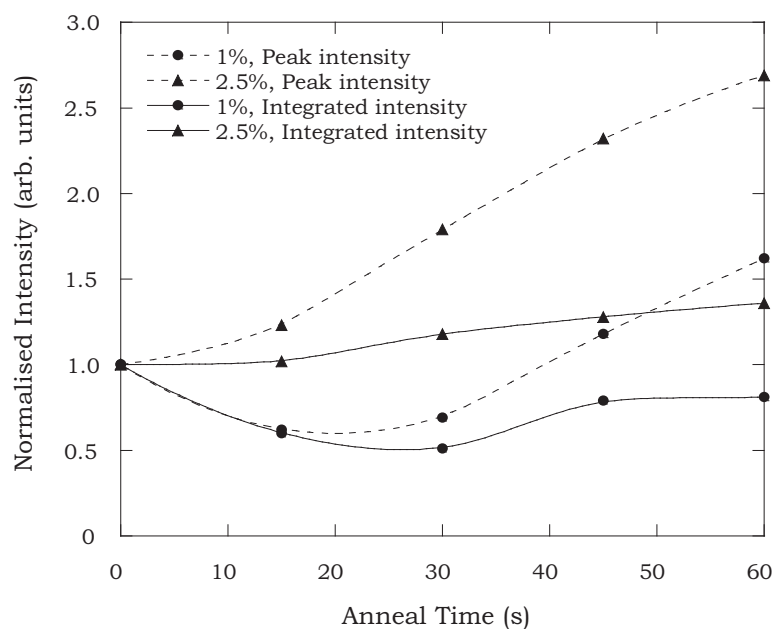


Fig. 4. 15K PL peak intensity and integrated intensity data for the 1.0% and 2.5% GaNAs MQW samples for different anneal times.

Something which seems to have received less attention in the published literature, but which is also an important consideration, is the limit to which annealing can improve PL efficiency. If the degradation of PL intensity is related to defect density, then performance enhancement through the annealing-out of defects is certainly limited. Additionally, the model suggested by Grenouillet *et al*. Grenouillet et al. (2002) to explain optical performance based on composition fluctuations has been demonstrated both theoretically and experimentally Grenouillet et al. (2002); Pan et al. (2000) to result in a limit beyond which improvement is negligible, although some papers have shown that 'extreme' annealing can also cause samples to degrade after passing through an 'optimal' state see Hierro Hierro et al. (2003), Gupta *et al* Gupta et al. (2003) and Xin *et al* Xin et al. (2000). The presence of hydrogen (which pacifies optically-active centers) can also confuse matters, since its incorporation during 'gas-source' and 'metal-organic' growth and subsequent out-diffusion during annealing can augment perceived improvements in optical efficiency Klar et al. (2003); v H G Baldassarri et al. (2001).

The work and the data presented here is insufficient to comment on annealing to 'extremes', although the behaviour of both peak and integrated intensity, illustrated in figure 4, seem to indicate a fall-off in the rate of increase with anneal time. The initial drop in both peak and integrated intensity for the 1.0% samples might also suggest that localised excitonic emission is the main source of emission in the as-grown 1.0% samples, but is quickly annealed out in favour of band-edge emission from the uniform alloy. However, the underlying problems with the morphology and defect density of both sets of samples are still sufficient to prevent RT emission, see figure 5.

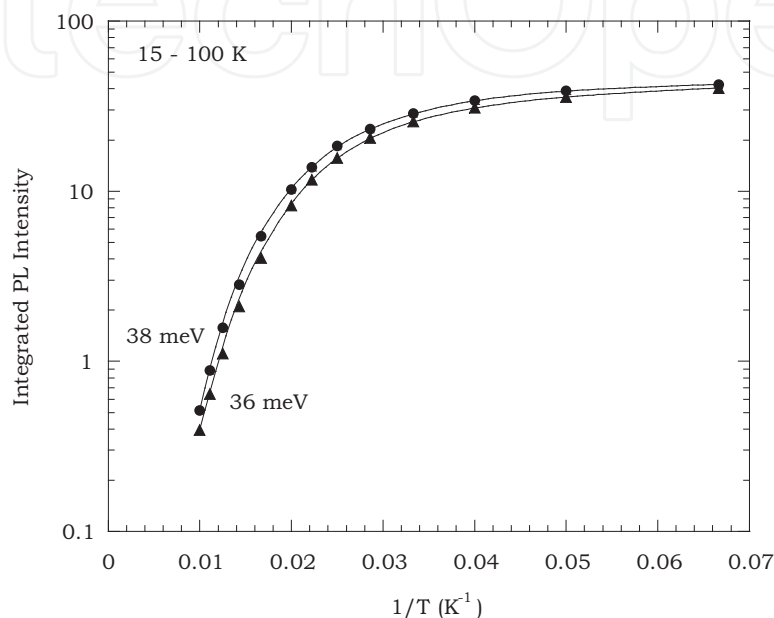


Fig. 5. Arrhenius plot for a GaN_{0.025}As MQW sample after annealing for 30s (●) and for 60s (△) at 800°C.

The Arrhenius plot of the 2.5% nitrogen samples shows that emission begins to fall off at around 35 K, dropping by around two orders of magnitude by 100 K. The activation energy of the thermal loss mechanism is 38 meV after 30s and 36 meV after 60s, and a decrease from 41 to 38 meV is also observed for the 1.0% samples after a similar anneal. These values are comparable with those given for both GaNAs and GaInNAs MQW samples Pomarico et al. (2002); Toivonen et al. (2003a), although relatively few papers analyse GaNAs samples before and after annealing in such a manner.

The observed consistent drop in the activation energy upon annealing might indicate a loss of nitrogen from the wells. If we were to assume that the blue shift is entirely due to a change in overall nitrogen composition of the wells then, according to figure 6, such a blue shift would be consistent with a decrease in nitrogen composition of about 0.1%. This result is more than two orders of magnitude smaller than the same result given by Wang et al Wang et al. (2002). But this slight reduction in N-concentration (around 0.1%) is unlikely to be the cause of the large blue shifting and improvements in emission. In any case, the evidence published on the diffusion of nitrogen (or lack thereof) from dilute nitride layers is not conclusive, and seems to be strongly-dependent on the composition/miscibility of the alloy and defect density Albrecht et al. (2002); Loke et al. (2002); Peng et al. (2003).

Illustrated in figure 7 is the XRD rocking curves from samples GaNAs₂₁₋₂₄, which shows no evidence of significant changes in the two structures after the rapid thermal annealing

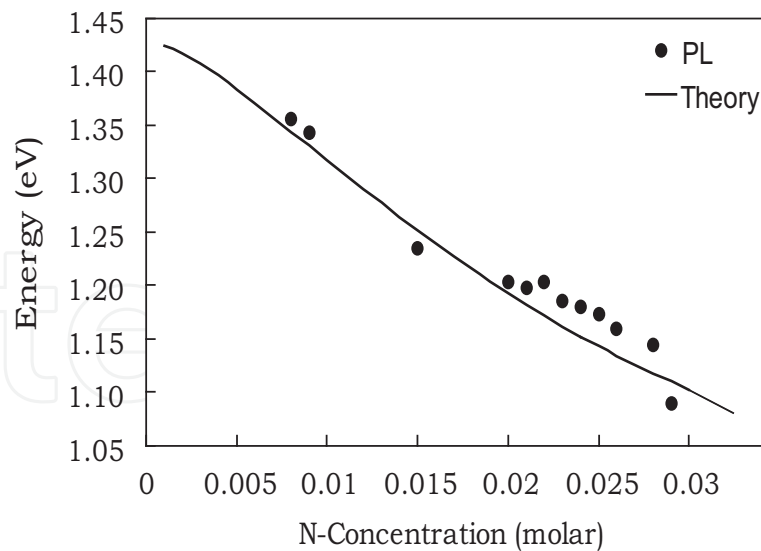


Fig. 6. Theoretical (Solid line), for a well width of 70\AA and experimental (Circles) optical transitions in $\text{GaN}_y\text{As}_{1-y}$ MQW annealed samples, with varying nitrogen concentrations determined from low temperature PL measurements.

(within the errors of the model). The main finding was that the structures grown were smaller than had been intended due to a lower than expected growth rate. This suggests that neither nitrogen out-diffusion from the wells, nor changes in well thickness, are likely to be responsible for the blue shifting and intensity enhancement demonstrated by this set of samples as a result of annealing. However, there is insufficient information here to comment on whether the changes are related to a general reduction in defect density and improvement in alloy uniformity, or to an improvement in morphology and/or compositional uniformity at the interfaces Li, Pessa, Ahlgren & Decker (2001); Toivonen et al. (2003a;b).

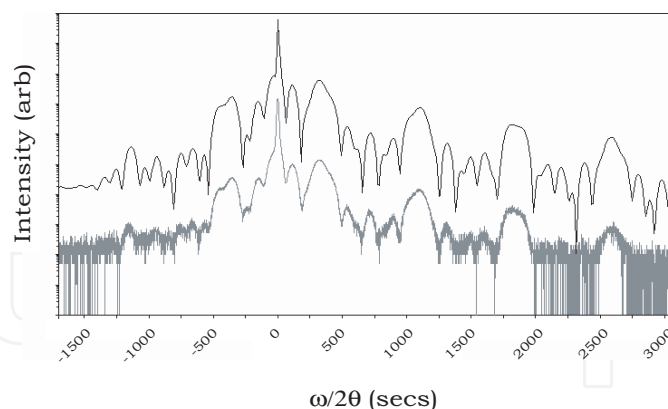


Fig. 7. Measured (lower) and simulated (upper) XRD rocking curves for as-grown 'GaNAS24'. The simulation is based on a five-period $\text{GaN}_{0.025}\text{As}/\text{GaAs}$ MQW structure with 6.5 nm-thick QWs, 18.8 nm-thick cladding layers and a 70 nm GaAs cap.

Another interesting feature of the PL spectra for the 1.0% samples (at low T) is that of the prominent low-energy tail, observed by both Buyanova et al. Buyanova, Pozina, Hai, Thin, Bergman, Chen, Xin & Tu (2000) for MQW samples and by Wang et al. Wang et al. (2003) for 100 m-thick $\text{GaN}_{0.0145}\text{As}$ epilayers. Attempts have been made to explain the origins of this feature with particular reference to localised excitons (LEs),

initially due to the exponential shape of the tail, even though the origin of this localisation is not fully understood. In some cases, PL spectra measured as T is increased from ~ 10 to 300 K display two peaks, one of which diminishes with increasing T (characteristic of LE emission) and the other of which increases with T (characteristic of free exciton (FE) emission) Buyanova et al. (2002); Mair et al. (2000); Shirakata et al. (2002). In addition, the S-shaped temperature dependence of the peak emission wavelength for GaNAs samples also suggest that localised excitons dominate recombination at low T in dilute nitrides Hierro et al. (2003); Mazzucato et al. (2003); Pomarico et al. (2002).

To date, the reasons offered for localisation at low T relate to compositional fluctuations within the lattice Buyanova et al. (2003); Grenouillet et al. (2002); Hong & Tu (2002); Kent & Zunger (2001a), or to the presence of point defects. These point defects can take the form of low-level contaminants and vacancy defects Li, Pessa, Ahlgren & Decker (2001); Toivonen et al. (2003b), and of N-related defects such as interstitials and complexes Ahlgren et al. (2002); Li, Pessa & Likonen (2001); Masia et al. (2003) (which are shown to increase with N-concentration) and ion-induced damage at the interfaces Ng et al. (2002); Pan et al. (2000). What is clear from published material is that the annealing of GaInNAs samples removes interstitial nitrogen and other non-radiative centers, thereby improving alloy homogeneity, enhancing PL efficiency and reducing the prevalence localised excitons.

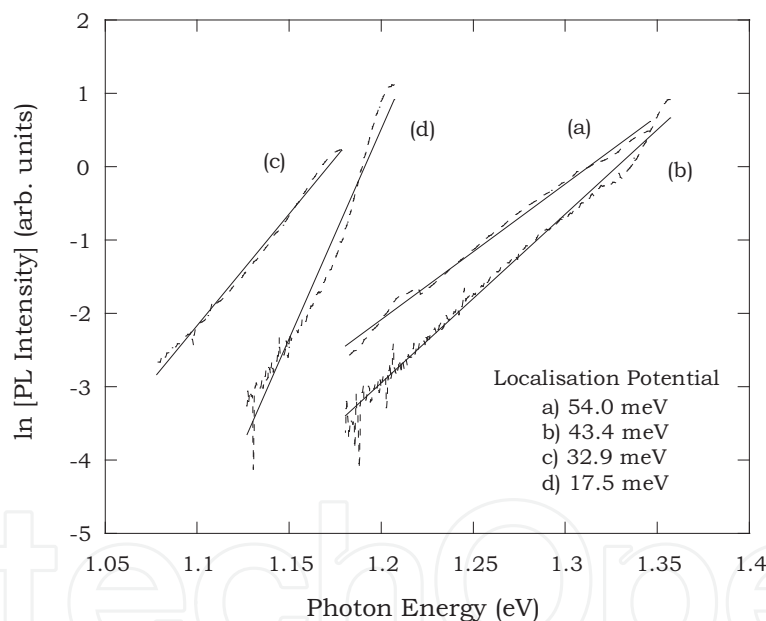


Fig. 8. Natural-log plots of low-E halves of PL spectra (dotted lines) and linear fits (solid lines) for (a) GaNAs23 (as grown), (b) GaNAs23 (60 s anneal), (c) GaNAs24 (as grown), and (d) GaNAs24 (60 s anneal). An estimate of the localisation potential is given by the reciprocal of the gradient.

In order to estimate the localisation potential responsible for the exponential tails seen in figures 2 and 3, the low-E side of each spectrum was plotted on a natural log scale, see figure 8. These estimates are very close to one made by Buyanova et al. for a virtually-identical structure Buyanova et al. (1999), and would seem to indicate that the localisation potential decreases with a 60 s RTA at 800°C for both samples, although the data for GaNAs24 does not

fit as well as for that of GaNAs₂₃. This might be expected, looking at figures 2 & 3, since the exponential tail is much more prominent for GaNAs₂₃ than for GaNAs₂₄.

2.2 Annealing of the quaternary GaAs-based dilute nitride: GaInNAs

Even though by nature a more complex system than GaNAs, being a quaternary RTA in GaInNAs and its mechanisms are better understood and the general interpretation of experimental observations are less contradictory. The presence of In seems to be the key in this alloy. During the growth process, chemical bonding aspects dominate at the surface which favour GaN bonds instead of InN bonds Kurtz et al. (2001). This surface state is frozen in during the non-equilibrium growth process. In contrast to the surface, In-rich nn-configurations of N are favoured in bulk at equilibrium due to the dominance of local strain effects. Therefore, the frozen non-equilibrium bulk state can be transformed into the equilibrium bulk state by annealing under appropriate conditions. Annealing GaInNAs leads to a rearrangement of the N-sites favouring In-rich nn-environments. Depending on the growth conditions, as well as annealing procedure, this presents one of the main contributions to the large blue shift after annealing, which is observed in the PL of Ga_{1-y}In_yN_xAs_{1-x} structures grown either by MOVPE or by MBE Masia et al. (2003); Moison et al. (1989). Further experimental and theoretical evidence for this process was given in Wagner et al. (2003) and Seong et al. (2001). Combining Monte Carlo and pseudo-potential supercell studies, Kim and Zunger found that annealing of GaInNAs causes changes in the nn-configurations of N towards In-rich environments and results in a blue shift of the band gap. Kurtz et al showed by FT-IR vibrational spectroscopy that annealing of Ga_{0.94}In_{0.06}As_{0.98}N_{0.02} converts nn-environments of N from 4Ga to 3Ga and 1In. X-ray photoelectron spectroscopy have to date revealed that nitrogen exists in two bonding configurations in not-annealed material, a GaN bond and another nitrogen complex in which N is less strongly bonded to gallium atoms. Annealing removes this second nitrogen complex. A combined nuclear reaction analysis and channeling technique showed that not annealed GaNAs contains a significant concentration of interstitial nitrogen that disappears upon anneal. It is believed that this interstitial nitrogen is responsible for the deviation from Vegard's law and the low luminescence efficiency of not annealed GaNAs and GaInNAs quantum wells.

The low luminescence efficiency in not-annealed GaInNAs, again, indicates the existence of nonradiative recombination centers or traps. Therefore annealing increases the luminescence efficiency by decreasing the concentration of these centers. Saito *et al* Saito et al. (1998) Xin *et al* Xin et al. (1999) and Geisz *et al* Geisz et al. (1998) postulated that this trap was due to hydrogen impurities. They observed that during the growth of nitride-arsenides by metal-organic chemical vapor deposition (MOCVD) or gas source molecular-beam epitaxy hydrogen supplied in the group V gas sources is incorporated. They also observed changes in the hydrogen concentration profile when annealing. However, Spruytte *et al* Spruytte et al. (2001b) group and other people growing nitride-arsenides by solid source MBE (such as the group I am involved with) using an rf plasma Miyamoto et al. (2000) observed the same increase of luminescence efficiency with annealing with almost no hydrogen present. Hence, despite the recent laser successes, there is still significant work remaining to tame GaAs-based dilute nitride materials system in order to realize the full wavelength range of high-performance optoelectronic emitters. Most critically the strong impact of annealing on the material properties clearly indicate that, still, the epitaxial growth of these alloys is not yet fully mastered. Some aspects such as, to cite but a few, the effect of plasma species on

the crystal quality during MBE growth, N segregation, phase separation, ordering, remain to be explored. For all growth techniques there appear to be a need to further work on N-sources. The fine structure of the band gap of GaInNAs, and the metastability caused by different N-environments, requires further studies. The implications on the band alignment of heterostructures containing GaInNAs, as well as on the properties of lasers containing this quaternary alloy, need to be discussed. Also transport properties of these alloys should be investigated in more details in connection with epitaxial growth conditions. Most work to date has focused on low N-content alloys. the growth of high-quality high-N-content alloys for fundamental as well as applied purposes remains a real challenge.

2.3 Alternative dilute nitride emitting structures: SPSL structures

Further to our studies above, in order to gain a better understanding of the issues raised above we have also started to investigate short period super lattice (SPSL) structures of GaInNAs system. The SPSL growth method provides a simple way to tune the N concentration in ternary, GaNAs QWs as well as the In concentration in the quaternary, GaInNAs QWs. The low temperature PL spectra of a $7(\text{GaN}_{0.025}\text{As})_5 6(\text{GaAs})_{6.4}$ SPSL and the equivalent $70 \text{ GaN}_{0.01}\text{As}/\text{GaAs}$ QW, where the parameters stated are determined through XRD measurements, low temperature PL is illustrated in figure 9.

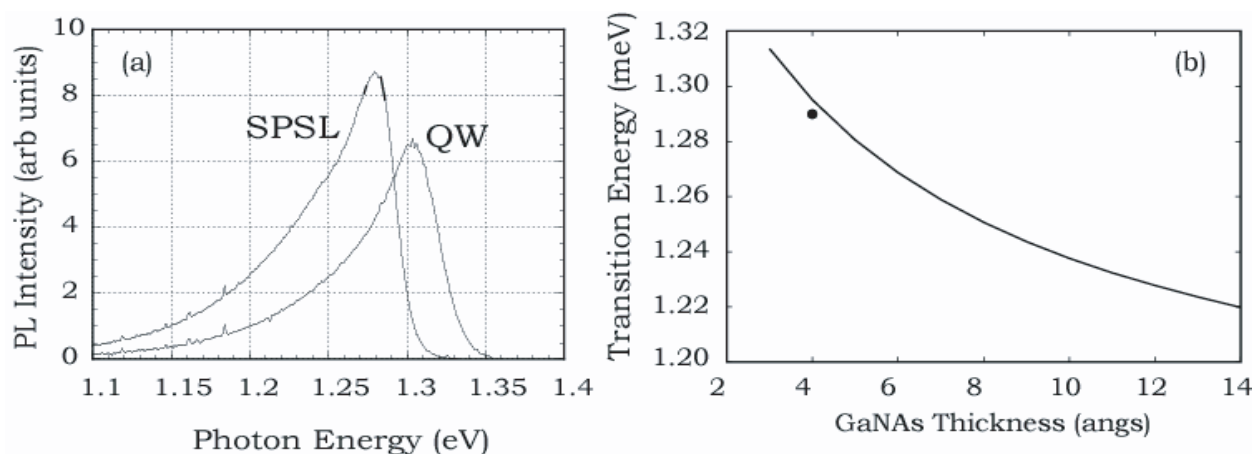


Fig. 9. (a) 15K PL of $7(\text{GaN}_{0.025}\text{As})_5 6(\text{GaAs})_{6.4}$ SPSL and $80 \text{ GaN}_{0.01}\text{As}/\text{GaAs}$ QW samples. (b) The calculated transition energy of $7(\text{GaN}_{0.025}\text{As})_m 6(\text{GaAs})_n$ SPSL structure vs. $\text{GaN}_{0.025}\text{As}$ thickness, m . The $7(\text{GaN}_{0.025}\text{As})_5 6(\text{GaAs})_{6.4}$ SPSL measured PL-peak is shown by the dark circle.

The PL intensity of the SPSL sample is stronger than that of the bulk layer, as reported also by Hong *et al* Hong et al. (2002; 2001). The PL-peak position, however, is slightly smaller than that of the bulk layer. This is in accordance with our transition energy calculations of figures 6 and 9(b), by comparing their relative positions on figures 6 and 9(b) respectively. The SPSL calculation of figure 9(b) is based on the propagation matrix algorithm Jalili et al. (2004), see chapter 5.

Therefore a better way to improve the luminescence efficiency (material quality) of $\text{III-N}_y\text{-V}_{1-y}$ alloys, would be that instead of growing the alloy GaInNAs with a random spatial distribution of atoms of the group III elements, a super-lattice (SL) based on the binary compound InAs and the ternary GaNAs should be grown. This would result in a precise arrangement of group III elements and separation of In and N into distinct, separate, layers

Hong et al. (2001). There would, of course, be significant strain to be accommodated due to the lattice mismatch of $\sim 6\%$ between InAs and GaAs and this would restrict the thickness of the layers forming the super-lattice Gerard et al. (1989); Hasenberg et al. (1991); Jang et al. (1992); Moreira et al. (1993); Toyoshima et al. (1990; 1991). An obvious way to reduce the strain and hence remove the bound on the layer thickness would be to use two ternary alloys GaInAs and GaNAs. Certainly, this could be done. The advantage of the binary/ternary combination is that we remove the need to control both In and nitrogen, needing only to control the nitrogen.

2.3.1 (Short-period) Super-lattice structures

The concept of the semiconductor "super-lattice" (SL) was introduced by Leo Esaki, Esaki & Tsu (1970) to describe a crystalline structure with a periodic one-dimensional structural modification. This was achieved by growing, epitaxially and sequentially, multiple thin layers of two semiconductor materials of similar crystal structure but distinctly different energy band-gaps. In this paper we wish to develop and apply techniques to predict the optical properties of such super-lattices (SL) particularly short period super-lattices (SPSL). We aim to use this information to design and fabricate PPSL structures which are optically equivalent to structures formed using the quaternary III-N-V random alloy systems, Hong *et al* Hong et al. (2002; 2001), which will be our main topic for the rest of the current chapter.

3. The idealised super-lattice and its limitations

The electronic and optical properties of PPSL structures have usually been studied by considering an infinite number of identical layers stacked within the same semiconductor structure, and positioned periodically to form a super-lattice Sai-Halasz et al. (1977). The basic SL structure is illustrated in Fig. 10(a), where each period, or unit cell, consists of one well region with width, d_A , and a barrier region of width, d_B . The period of the super-lattice is $d = d_A + d_B$. The host materials, labeled A and B, are the binary (InAs) and ternary (GaNAs) semiconductors respectively. Other configurations using the ternary, GaInAs, and the ternary GaNAs, structures are also possible Hong et al. (2002; 2001).

The Kronig-Penny model of the super-lattice, which is based on the Bloch theorem, is an idealized model. Any practical structure will have a finite number of period and, as shown in Fig. 10(b), is often bound by a wider band-gap semiconductor (labeled 'C' in Fig. 10(b)). Indeed it is quite possible to consider the structure shown in Fig. 10(b) to be one element of a structure in which the structure is repeated in an analogous way to the formation of multiple quantum wells. We will consider the modeling of this (short-period) super-lattice later. At this point, however, we will discuss the model of the idealized structure, considering it as a limiting case which our finite model must tend to as the number of periods becomes large. To determine the band-structure of the SL structure (a), we consider the potential within a period $0 < z < d$ to be given by

$$V(z) = \begin{cases} V_A & 0 < z < d_A \\ V_B & d_B < z < d \end{cases} \quad (1)$$

and

$$V(z + nd) = V(z), \quad \text{for any integer } n. \quad (2)$$

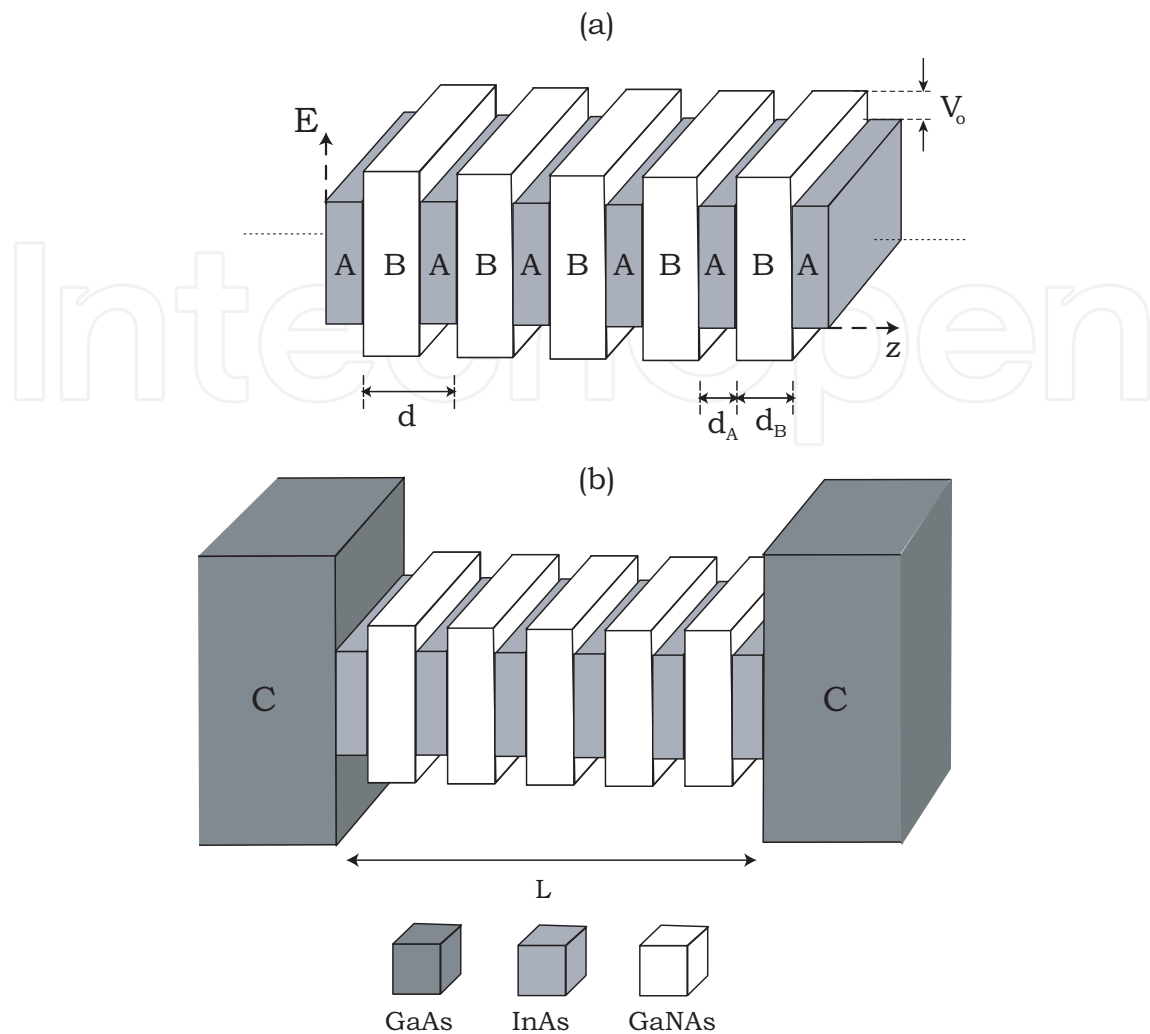


Fig. 10. Schematic representation of the conduction and valence band edge profile of (a) a SL structure of semiconductors A and B (or in-short $(A)_{d_A}(B)_{d_B}$), showing wells of width d_A alternating periodically with barriers of width d_B and differential height V_0 , to form a SL of period $d = d_A + d_B$. (b) SL structure of finite length L , confined by semiconductor C, GaAs, i.e. SPSL.

Within such a structure the electrons and holes experience a periodic potential, which is unbounded in the same way as we assume for a bulk crystal. This implies that the electron or hole wave-functions are no longer localised but extend through-out the lattice. Electrons are therefore equally likely to be found in any of the wells in the super-lattice. Electrons in such a structure are said to occupy "Bloch states".

$$\Psi_I(z + d) = e^{iqd}\Psi_I(z) \quad (3)$$

The energy dispersion curve for the SL, $E(q)$, will be restricted to the first Brillouin zone of the SL, i.e. $-\pi/d \leq q \leq \pi/d$. The SL (or Bloch) wavevector, q , is orientated along the crystal growth direction, which we have taken to be the z -axis. The SL dispersion curves representing the energy E of a particle as a function of its wavevector, q , are obtained from the Kronig-Penny expression.

$$\cos(qd) = \cos(k_A d_A) \cos(k_B d_B) - \frac{k_A^2 + k_B^2}{2k_A k_B} \sin(k_A d_A) \sin(k_B d_B) \quad (4)$$

We use the nomenclature $(\text{InAs})_m (\text{GaN}_y\text{As})_n$ to specify a SL in which m mono-layers of the binary alloy and n mono-layers of the ternary constitute the basic lattice which is repeated to form the super-lattice. Calculations of the band-structure are shown below in Fig. 11(a) and (b) for $m=4, n=4$; $m=4$, and $n=9$; and for two different nitrogen compositions.

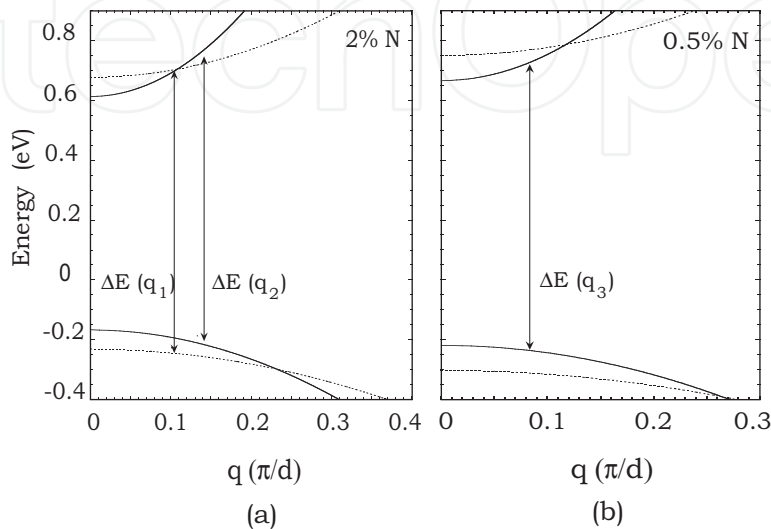


Fig. 11. Band structure calculations of $(\text{InAs})_4 (\text{GaN}_y\text{As})_4$, solid line, and $(\text{InAs})_4 (\text{GaN}_y\text{As})_9$, dashed line, SLs. (a) GaNAs with 2% N (b) GaNAs with 0.5% N.

By analogy with bulk and QW energy dispersion relations, we should be able to predict the thickness of a SPSL structure by analysing the energy wave-vector dispersion plot of an equivalent SL-structure, i.e. the same unit cell structure, in the reciprocal space. This can be done from the definition of k -vector, in the k -space the propagation vector, which is basically, assuming $\Psi(z) \rightarrow 0$ at end points, the simple quantum mechanical expression

$$\begin{aligned} E &= \frac{1}{2m^*(E)} \hbar^2 |q|^2 \\ &= \frac{1}{m^*(E)} \hbar^2 \frac{2\pi^2}{L^2} (n_x^2); \quad n_x = 0, \pm 1, \pm 2 \dots \end{aligned} \quad (5)$$

Relating the wave-vector, $k(\equiv q)$, and the transition energy, $\Delta E(k)$. Pictorially, by using the energy wave-vector dispersion diagram of a SL structure, illustrated schematically in Fig. 10(a), we would want to estimate the thickness, L , of a SPSL structure, illustrated schematically in Fig. 10(b), which have the same unit cell and transition energy. The energy wave-vector dispersion of $(\text{InAs})_4 (\text{GaN}_{0.02}\text{As})_9$ SL structures for two different N compositions of 0.5% and 2% are illustrated in Fig. 11(a) and (b) respectively. The two transition energies, $\Delta E(q_1)$ and $\Delta E(q_2)$ both correspond to $1.3 \mu\text{m}$ emission, shown in Fig. 11(a). However as the wave vector in the latter transition is larger, then the corresponding SPSL structure will have a smaller overall length in comparison. This is deduced from Eq 5.

4. The short period super-lattice

Before we proceed to the details of the propagation matrix calculation of the optical transitions in a SPSL, we need to consider the properties of the binary (InAs) and ternary (GaNAs) alloys that form the SPSL. There are two distinct issues we need to address. The first is simply the modeling of the bulk properties of these materials, particularly when there is considerable strain at the interface with say, GaAs. The second issue is the need to determine the band off-set arrangement both between InAs and GaNAs and GaNAs and GaAs.

We start with the binary alloy InAs, this is a narrow gap III-V semiconductor, so when considering optical transitions, band non-parabolicity is important and must be accounted for. We used the 3-band Kane Hamiltonian to investigate the band-edge electronic description of bulk InAs-GaAs, where the lattice mismatch is accommodated by biaxial compressive strain within the InAs layer. To model the GaNAs, we use the band-anti-crossing (BAC) model to explain the unusually strong band-gap reduction of GaAs through the replacement of only a few percent of the arsenic atoms by nitrogen Shan et al. (2001); Weyers et al. (1992). The good agreement between a 5-band (10 including spin) k.p and the BAC model, confirms the validity of this two band model at the band-edge O'Reilly et al. (2002). In this model, the nitrogen atoms form a flat and almost dispersionless band, resonant with the GaAs conduction band, but, which also interacts with the GaAs conduction band minimum. This interaction leads to the formation of two bands of mixed GaAs-nitrogen character. The lower band is shifted downwards with respect to the GaAs conduction band-edge by > 100 meV for each percent increase of nitrogen concentration. The new conduction band minimum is strongly non-parabolic. To take account of this, and the non-parabolicity of the valence band, we have used the modified Kane Hamiltonian, with the inclusion of the nitrogen.

The Hamiltonian, which includes the off-diagonal matrix elements linking the ψ_N , ψ_C and ψ_{lh} , ψ_{so} basis states, is written as

$$\begin{bmatrix} E_N & V_{NC} & P_N k_z & 0 \\ V_{NC} & E_C & -i\sqrt{\frac{2}{3}}P_K k_z & i\sqrt{\frac{1}{3}}P_K k_z \\ P_N k_z & i\sqrt{\frac{2}{3}}P_K k_z & \delta E_s & -\sqrt{\frac{1}{2}}\delta E_s \\ 0 & -i\sqrt{\frac{1}{3}}P_K k_z & -\sqrt{\frac{1}{2}}\delta E_s & E_{so} \end{bmatrix} \quad (6)$$

Where the nitrogen dependant terms are defined as

$$\begin{aligned} E_C &= E_g^{GaAs} - (1.55 - 3.88)y \\ E_N &= 1.65 - (3.89 - 3.88)y \\ V_{NC} &= -2.4\sqrt{y} \end{aligned} \quad (7)$$

The nitrogen concentrations, y , in molar units, are extremely small, only a few percent. δE_s , and E_{so} are the light-hole and the spin-orbit splitting band-edges respectively. The heavy-hole band is decoupled from the rest of the bands. The heavy-hole band-edge is set at zero. The coupling term, the matrix element P_N , in the Hamiltonian above is $\sim 10\%$ of P_K , the Kane matrix element, as reported by O'Reilly et al O'Reilly et al. (2002). However, others suggest that P_N is about an order of magnitude smaller than this Linsay (2002). Therefore in view of there being no consensus over the value of P_N and also the general difficulty in determining its value, it is therefore best to set the k-dependant N-related terms to zero. The determinant

equation $|H_{Kane,N} - EI|$ then gives the following dispersion relation within the vicinity of the band edges

$$k_z^2 = \frac{3}{P_K^2} \frac{(E - E_N)(E - E_C)[(E - \delta E_s)(E - E_{s0}) - \frac{\delta E_s^2}{2}]}{(E - E_N)[3E + \delta E_s - 2E_{s0}]} \quad (8)$$

$$- \frac{V_{NC}^2 [(E - \delta E_s)(E - E_{s0}) - \frac{\delta E_s^2}{2}]}{(E - E_N)[3E + \delta E_s - 2E_{s0}]}$$

The lattice mismatch between bulk GaNAs and GaAs is accommodated by biaxial tensile strain within the GaNAs layer. Plots of band structures of InAs-GaAs and GaN_{0.02}As are illustrated in Fig. 12(a) and (b) respectively.

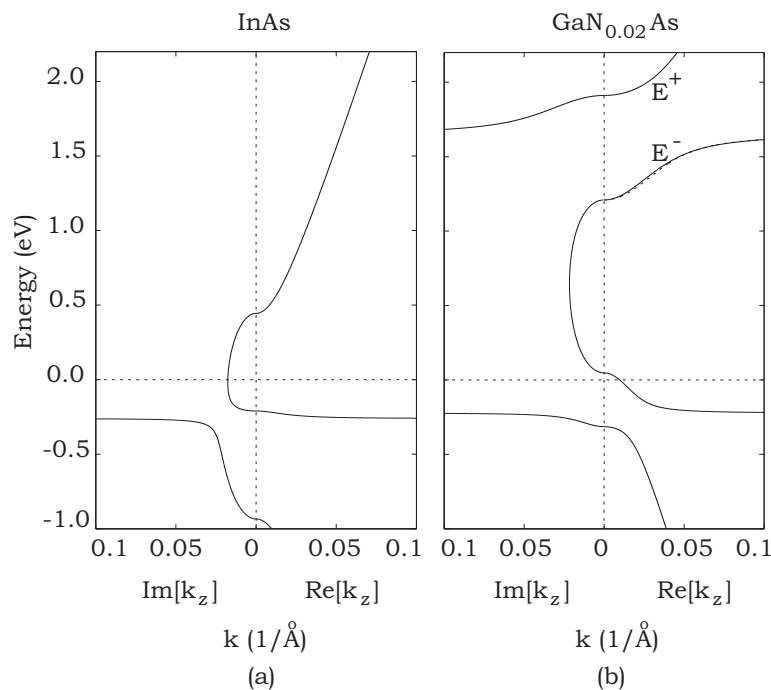


Fig. 12. Illustration of calculated, Kane description, dispersion relations of real and imaginary wave-vectors in InAs and GaN_{0.02}As semiconductors, corresponding to 6.67% compressive and 0.53% tensile strains respectively. The dashed line is based on the BAC Shan et al. (1999) model.

Except for the band-gap energy, the electron effective mass, Skierbiszewski et al. (2000) the lattice constant and the valence band deformation potential, Raja et al. (2002) most parameters for GaN_yAs_{1-y} are obtained by a linear interpolation between the parameters of the relevant binary semiconductors given in table 2.

Moving to the discussion of the band off-set issue, we note that the presence of nitrogen atoms is assumed to influence predominantly the host conduction band, with the valence bands remaining largely undisturbed. Following this model one might therefore expect the band-gap mismatch between the well and barrier material in GaN_yAs_{1-y}/GaAs heterostructure to show up predominantly in the conduction band off-set, with the valence-band offset being zero or negative. However, recent experiments suggest that

	GaAs	InAs	GaN	InP
$E_{g, RT}$ (eV)	1.424	0.36	3.2	1.344
$E_{g, LT}$ (eV)	1.519	0.41	3.39	1.424
E_p (eV)	25.7	22.2	25.4	16.7
Δ (eV)	0.34	0.32	0.015	0.11
a_o (Å)	5.6533	6.0584	4.503	5.8687
a_{gap} (eV)	-8.3768	-6.08	-7.8	-6.31
b (eV)	-1.7	-1.8	-1.9	-1.7
c_{11} (GPa)	181.1	83.29	293	10.11
c_{12} (GPa)	53.2	101.1	159	5.61
m_e^*/m_o	0.067	0.023	0.22	0.08
m_{hh}^*/m_o	0.5	0.4	0.8	0.6
m_{lh}^*/m_o	0.087	0.026	0.19	0.089
m_{so}^*/m_o	0.15	0.16		

Table 2. Parameters of GaAs (de Walle (1989)), InAs (de Walle (1989)), InP and GaN (de Walle (1989); Fan et al. (1996); Kim et al. (1996); Pearton (2000); Persson et al. (2001)) used in the calculations.

this might not be true Buyanova, Pozina, Hai & Chen (2000); Egorov et al. (2002). Latest results and measurements have determined that the band lineup in GaNAs-GaAs (for low N compositions) is of type I Buyanova, Pozina, Hai & Chen (2000); Egorov et al. (2002); Klar et al. (2002). InAs and GaAs are also expected to show a type I band line up de Walle (1989). However, to authors' knowledge, there is currently no information on band lineup of InAs-GaNAs heterostructure. Therefore, with GaAs band edges as the reference, we have lined up InAs and GaNyAs by lining up InAs/GaAs (60:40 in favour of CB) and GaNyAs/GaAs ($y = 0.02$, $\sim 90:10$ in favour of CB). The band diagram is illustrated in Fig. 13.

5. SPSL design & calculations: The propagation matrix approach

In this section we show how the Schrödinger equation for a one dimensional potential profile with an arbitrary shape, a SPSL in this case, (Fig. 10(b)), can be solved using a propagation matrix approach, similar to that used in electromagnetic wave reflection or guidance in a multilayered medium Kong (1990); Yeh & Yariv (1984). An arbitrary profile, $V(z)$ can always be approximated by a piece-wise step profile. In contrast to the conventional method, described above, where the Bloch condition must be employed to obtain the required translational symmetry of the problem Bastard & Brum (1986), a propagation matrix approach produces a more accurate energy band solution of a SPSL structure Ram-Mohan *et al* Ram-Mohan et al. (1988), since it provides an extra degree of freedom in space, z , to vary the, layer dependant, potential $V_l(z)$ accordingly. This is in contrast to the conventional method in which the layer dependant potential remains fixed and repeats itself infinitely over the SL

unit cell Bastard (1988). Of course, a SPSL structure should tend towards a SL structure with increasing period. One way of discovering exactly how many quantum wells or unit cells are required before a finite structure resembles an infinite one (i.e. a SL) would be to look at the ground state energy as a function of the number of periods within a SPSL structure.

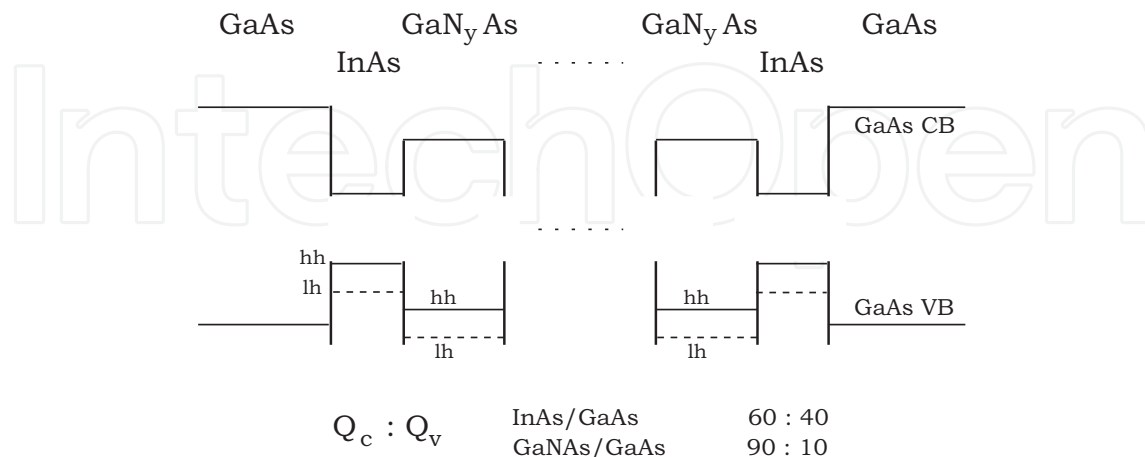


Fig. 13. Energy band line-up profile of GaAs/M(InAs)_{d_A}N(GaN_{0.02}As)_{d_B}/GaAs SPSL structure. lh and hh denote light and heavy holes, the conduction and valence band offsets, denoted by Q_C and Q_V respectively is determined to be 50:50 for InAs/GaN_{0.02}As.

A SPSL structure may consist of a number of heterostructures. As we know QWs are fabricated by forming heterojunctions between different semiconductors. From an electronic viewpoint, semiconductors are different because they have different band structures and, hence, band gaps. Apart from the bandgap, there are other properties which are also different in semiconductors, such as the dielectric constant, the lattice constant and, what is considered as the next most important quantity, the effective mass. In general the calculation of static energy levels within QWs should account for the variation in the effective mass across the heterojunction under appropriate boundary conditions. The boundary conditions on the envelope functions can be obtained by integration of the coupled differential equations across an interface. This problem has been previously addressed in the literature, Johnson *et al*, also Bastard *et al* and Taylor *et al*, these can be stated as requiring the continuity of both

$$\psi_{l,n}(E, z) \quad \text{and} \quad \frac{1}{m_{l,n}^*(E, z)} \frac{\partial}{\partial z} \psi_{l,n}(E, z) \quad (9)$$

across a heterostructure interface. Where $m_{l,n}^*(E, z)$ and $\psi_{l,n}(E, z)$ are the energy dependant effective mass and envelope coefficients in layer 'l' and band 'n', which we will look at in detail in chapter 2.

Within a multilayer structure, for a given energy, the envelope function in each layer can be written as a sum of forward and backward traveling waves

$$\psi_l(z) = A_l e^{ik_l(z-z_l)} + B_l e^{-ik_l(z-z_l)}, z_{l-1} \leq z \leq z_l \quad (10)$$

Where the wavevector k_l is given by the auxiliary equation for each layer and is expressed as

$$k_l^2 = \frac{2m_l^*(E, z)(E - V_l(z))}{\hbar} \quad (11)$$

Applying the boundary conditions of Eq. (9) a general form of a propagating matrix at an interface between layers l and l' is obtained as

$$\Pi_{l \rightarrow l'}(E) = P_l D_l^{-1} D_{l'} P_{l'} \quad (12)$$

where D_l , the transition matrix, which is obtained from the boundary conditions, and P_l , the propagating matrix, are defined as

$$D_l = \begin{pmatrix} 1 & 1 \\ \frac{k_l}{m_l^*(E,z)} & -\frac{k_l}{m_l^*(E,z)} \end{pmatrix}, \quad P_l = \begin{pmatrix} e^{ik_l z_l} & 0 \\ 0 & e^{-ik_l z_l} \end{pmatrix} \quad (13)$$

Therefore the matrix $P_l D_l$ takes us from layer $l + 1$ to l . For a large number of layers, the propagation matrix for each layer can be linked forming the propagation matrix of the whole structure

Imposing the relevant boundary conditions, (i.e. $\psi(z) \rightarrow 0$ as $z \rightarrow \pm\infty$) the wavefunction must tend toward zero into the outer barriers (GaAs in this case), and the coefficients of the growing exponentials must be zero. Therefore

$$\begin{pmatrix} A_N \\ 0 \end{pmatrix} = \begin{pmatrix} \Pi_{11}(E) & \Pi_{12}(E) \\ \Pi_{21}(E) & \Pi_{22}(E) \end{pmatrix} \begin{pmatrix} 0 \\ B_0 \end{pmatrix} \quad (14)$$

Eq. (14) implies that for nontrivial solutions, we must have the eigenequation above satisfy,

$$\Pi_{22}(E) = 0 \quad (15)$$

SPSLs are conventionally defined by the number M of interfaces of InAs grown upon GaNAs, and the number N of interfaces of GaNAs grown upon InAs, with the numbers m and n , measured in Angstrom (\AA), which define thicknesses of InAs and GaNAs layers respectively. Jang et al. (1992); Moreira et al. (1993); Toyoshima et al. (1990) The short form of the expression is $M(\text{InAs})_m N(\text{GaNAs})_n \equiv N[(\text{InAs})_m (\text{GaNAs})_n] + (\text{InAs})_m$. Therefore a SPSL of N periods consists of ' N ' GaN_yAs layers and ' $N+1$ ' ($=M$) InAs layers. In this case the SPSL structure equivalent to a single quantum well of the random alloy 8.5 nanometers thick and composition $\text{GaIn}_{0.35}\text{N}_{0.015}\text{As}/\text{GaAs}$, is obtained by imposing the molar composition ratios of III-N_y-V_{1-y} constituents onto SPSL layer thicknesses which would give us the numbers M , N , m and n , written in short form, as $7(\text{InAs})_4 6(\text{GaN}_{0.015}\text{As}_9)$ or $14(\text{InAs})_2 13(\text{GaN}_{0.015}\text{As}_{4.5})$. Hence the overall length of the SL is limited to what would be the typical dimensions of an 8.5 nm $\text{GaIn}_{0.35}\text{N}_{0.015}\text{As}/\text{GaAs}$ QW, which places the band-edge (0.95eV) at around 1.3 μm .

Fig. 14, illustrates, in plots (a) and (b), transition energies of $7(\text{InAs})_4 6(\text{GaN}_{0.02}\text{As})_n$ and $14(\text{InAs})_2 13(\text{GaN}_{0.02}\text{As})_n$ SPSLs, surrounded on either side by GaAs, as a function of barrier layer thickness, n , respectively. As expected, the transition energy is larger for the structure with smaller QW thickness, and for both structures, the transition energy levels off with increasing barrier thickness. Note that the points that correspond to the $7(\text{InAs})_4 6(\text{GaN}_{0.02}\text{As})_9$ and $14(\text{InAs})_2 13(\text{GaN}_{0.02}\text{As}_{4.5})$ SPSL structures in Fig. 14 plots (a) and (b) respectively, are indicated with a dashed line. As was predicted, the band edge transition is at 1.3 μm . Plot (a) of Fig. 15 is transition energy of an $M(\text{InAs})_3 N(\text{GaN}_{0.02}\text{As})_2$ SPSL as function of period, N , and plot (b) is that of the $M(\text{InAs})_4 N(\text{GaN}_{0.03}\text{As})_2$ SPSL, where in the latter case we have effectively lowered the barrier height by increasing the nitrogen concentration to 3% and the well thickness to 4 \AA respectively.

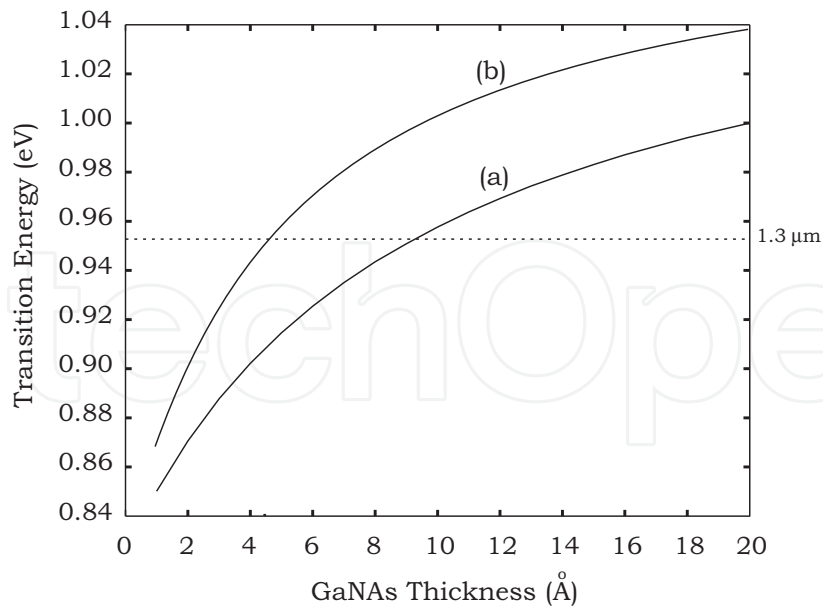


Fig. 14. Energy gap of InAs/GaN_{0.02}As SPSL structure as function of varying GaNAs (barrier) layer thickness (a) $7(\text{InAs})_{46}(\text{GaNAs})_n$ configuration (b) $14(\text{InAs})_{213}(\text{GaNAs})_n$ configuration.

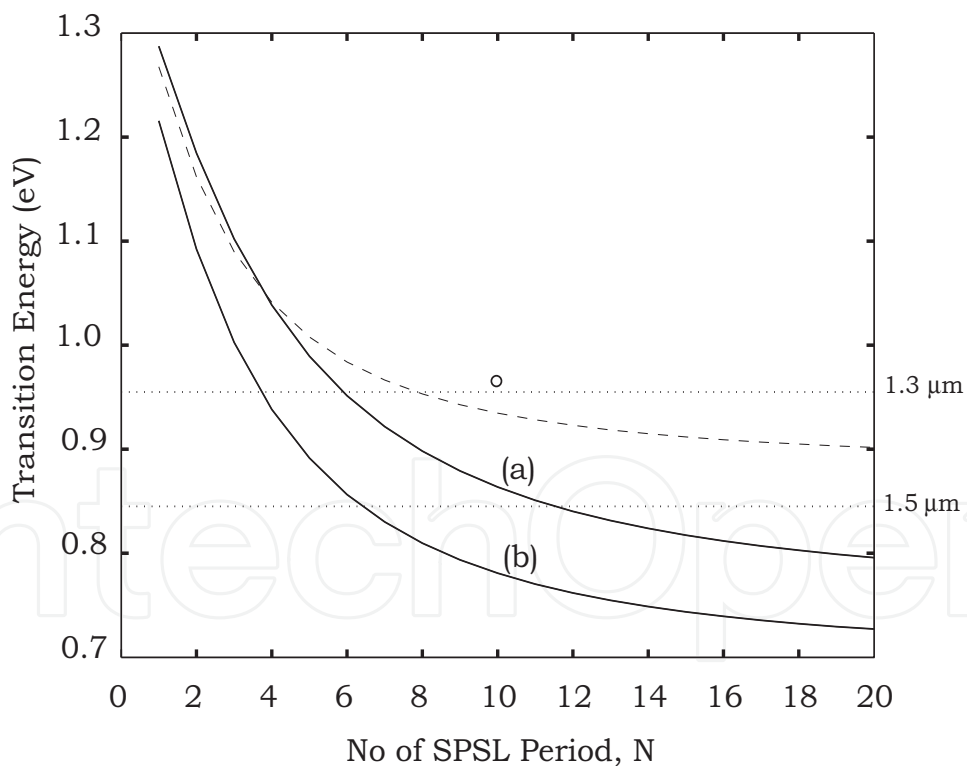


Fig. 15. The calculated transition energy plots of SPSL structures as function of SPSL-period, N . (a) $M(\text{InAs})_3N(\text{GaN}_{0.02}\text{As})_2$ and (b) $M(\text{InAs})_4N(\text{GaN}_{0.03}\text{As})_2$. The dotted line is the numerical result for the $M(\text{InAs})_3N(\text{GaN}_{0.023}\text{As})_{6.2}$ SPSL structure. The circle (o) is from Hong et al (needs reference in here) and is the experimental result for $10(\text{InAs})_39(\text{GaN}_{0.023}\text{As})_{6.2}$ SPSL annealed structure.

Therefore varying by the number of periods and/or barrier height within a SPSL structure, the position of the band edge can be modified significantly. For the plots it is clear that a structure which would absorb or emit at the important telecommunication wavelength of $1.5 \mu\text{m}$ can be achieved. We could equally reduce the potential barrier height of the cladding layer (GaAs in this case) by incorporation of In, in order to reduce the band edge to $1.5 \mu\text{m}$, since, due to limitations of strain, the InAs layer thickness, with a critical thickness, $h_c \leq 5$ Angstroms cannot be varied arbitrarily. As expected a larger number of SPSL periods, N , reduces the transition energy. The same pattern holds with a reduction in potential barrier height.

The following plots illustrate contour plots for various SPSL structures which emit or absorb light at $1.3 \mu\text{m}$. The contours in Fig. 16(i) indicate that by reducing d_B , tunneling across the barriers increases and leads to a reduction of the carrier energy within the wells. Therefore to make up for this reduction we need to increase the barrier height, V_o , or we must reduce the N concentration since the number of unit cells and the well width, d_A , are fixed. The two contour lines in the figure imply that if SPSL-period, N , is reduced in going from solid line contour to the dashed line contour, then the carrier energy is increased. Therefore thinner barriers or more nitrogen, are required to lower the barrier height, since d_A is fixed. Furthermore, for nitrogen concentrations of 0.5-1.5% the contour curvature is negligible with respect to N concentrations. This is particularly so for smaller numbers of periods, N . This is very significant considering that band gap variation in III-(N)-V systems is nonlinear with respect to the nitrogen concentration and is therefore very difficult to control even by sophisticated epitaxial growth techniques. Fig. 16(ii) illustrates $1.3 \mu\text{m}$ contour plots for fixed nitrogen concentration and well thickness. In this case an increase in barrier thickness, d_B , reduces the carrier energy within the wells, and therefore, to make up for this we would have to increase the number of periods. Going from the contour represented by a dashed line to the one represented in dotted line, the nitrogen concentration increases from 0.5% to 2% respectively. For higher nitrogen concentrations the barrier height V_o , is lowered implying that the carrier energy decreases. Therefore we would have to reduce the number of periods to make up for the carrier energy reduction. In Fig. 16(iii) the contours indicate that, since increase in number of periods lowers the carrier energy, the barrier height needs to be raised as d_A and d_B are both kept fixed. This is achieved by reducing the nitrogen concentration. The same pattern holds when barrier width, d_B , is reduced, as shown by the solid line of Fig. 16(iii). Again, as with contours of Fig. 16(i), the transition energy is not very sensitive to variations in nitrogen concentration for the smaller barrier width particularly for 2-3% nitrogen concentrations. This is in contrast to structures with comparatively larger barrier width (dashed line of Fig. 16(iii)) which leads to better control over nitrogen concentration in growth. These results, which are based on numerical models are in agreement with the predictions based on the SL model.

The results are very encouraging for design and fabrication of short period superlattices suitable for devices which emit or absorb light at $1.3 \mu\text{m}$ and also $1.5 \mu\text{m}$ of GaAs-based dilute nitrides. Specifically, more degrees of freedom are available for the design of nanostructure optoelectronic devices based on a given choice of materials. Structures can be engineered to vary the SPSL energy gap, by suitable choice of layer thicknesses, which can be atomically controlled using thin film crystal growth techniques such as MBE, as well as varying the number of SL period and layer composition. The proposals to use dilute nitride SPSL structures results in the separation of In and N and would over-come some of the key material issues limiting growth of III-N_y-V_{1-y} alloys. The growth of the binary and ternary configuration of GaInNAs SPSL should also provide better compositional control since the

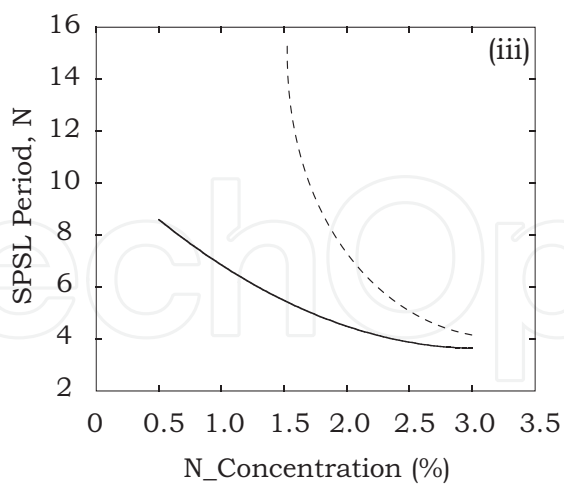
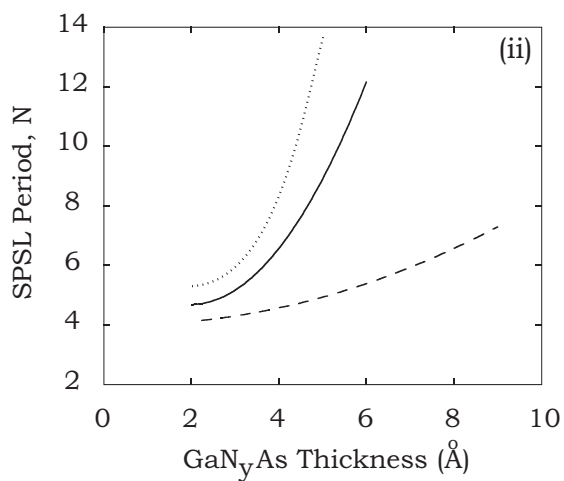
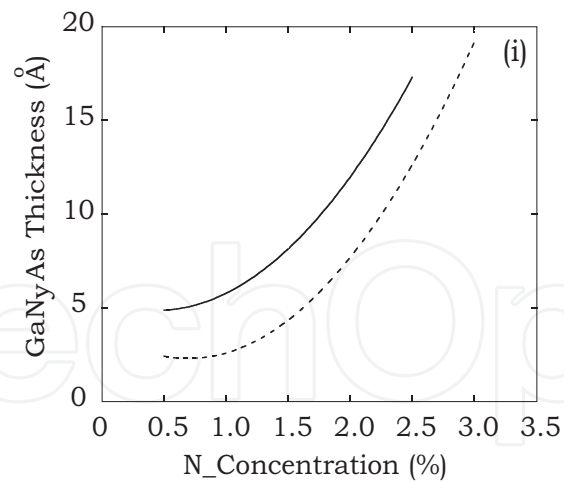


Fig. 16. $1.3 \mu\text{m}$ contour plots of (i) $4(\text{InAs})_413(\text{GaN}_y\text{As})_n$, solid line, and $7(\text{InAs})_46(\text{GaN}_y\text{As})_n$, dashed line, SPSLs vs. barrier width, n , and N-concentration, y . (ii) $M(\text{InAs})_4N(\text{GaN}_{0.005}\text{As})_n$, dotted line, $M(\text{InAs})_4N(\text{GaN}_{0.01}\text{As})_n$ solid line, and $M(\text{InAs})_4N(\text{GaN}_{0.02}\text{As})_n$, dashed line, SPSLs vs. number of periods and barrier width. (iii) $M(\text{InAs})_4N(\text{GaN}_y\text{As})_9$, dashed line, and $M(\text{InAs})_4N(\text{GaN}_y\text{As})_4$, solid line, SPSL structures as function of number of periods, N , and N-concentration, y .

incorporation of nitrogen will involve only one group III-element in each period of the structure. Also, since in SPSL structures the well/barrier width and therefore the period are in effect reduced to less than the electron mean free path, the entire electron system will enter a quantum regime of reduced dimensionality in the presence of nearly ideal interfaces, resulting in improved mobility within these structures. Therefore, design and growth of more efficient optoelectronic devices based on III-N_y-V_{1-y} systems should be possible. The current work on SPSL dilute nitride structures is very scarce. To authors knowledge apart from our group only one other has produced such work without any proper theoretical back up though. Therefore the potential is tremendous in this field with many possible directions in obtaining a better understanding of the important GaAs-based dilute nitride systems.

If dilute nitride materials are to prove their worth, then it must be demonstrated that they can be used to produce durable optoelectronic devices for use at 1.3-1.55 μ m applications. Unfortunately, a full understanding of the fundamental nature and behaviour of nitride alloys, especially during the annealing treatments that are required for optimum performance, continues to elude researchers. Certain trends have been identified qualitatively, such as that optimum anneal conditions depend on composition, and more specifically on (2D/3D) growth mode Hierro et al. (2003), on nitrogen content Francoeur et al. (1998); Loke et al. (2002), and on indium content for GaInNAs Kageyama et al. (1999), but 'optimum' annealing treatments continue to vary widely, according to growth method, growth conditions, structure and composition. We believe that SPSL structures have an important role to play in such studies. Therefore the priority should be to repeat the previous annealing study and try to obtain more information about the improvements seen during annealing. This could be done by measuring more-comprehensively the relationship seen in Arrhenius plots of integrated PL intensity vs. 1/T. Additionally, a series of experiments designed to find the optimum combination, duration and temperatures for in-situ and/or ex-situ annealing should be carried out, and repeated for SPSL active layers to determine whether such dilute nitride structures are capable of outperforming more-primitive MQW structures. These experiments should also provide another opportunity to investigate the optical performance of nitrides.

We made use of the transfer matrix algorithm based on the envelope function approximation (EFA). The results obtained demonstrated excellent agreement with those obtained experimentally so far, to authors knowledge, Hong *et al* Hong et al. (2001). Since the transfer matrix method is based on the EFA, it has the corresponding advantage that the input parameters are those directly determined by experimentally measured optical and magneto-optical spectra of bulk materials. The effect of additional perturbations, such as externally applied fields, built in strain in superlattices are easily incorporated into the **k.p** Hamiltonian with no additional analysis in the transfer matrix method. Furthermore the transfer matrix method provides a simple procedure to obtain the wavefunctions, which are particularly useful in evaluating transition probabilities.

6. References

- Ahlgren, T., Vainonen-Ahlgren, E., Likonen, J., Li, W. & Pessa, M. (2002). Concentration of interstitial and substitutional nitrogen in GaN_xAs_{1-x}, *Applied Physics Letters* 80: 2314–2316.

- Albrecht, M., Grillo, V., Remmele, T., Strunk, H. P., Egorov, A. Y., Dumitras, G., Riechert, H., Kaschner, A., Heitz, R. & Hoffmann, A. (2002). Effect of annealing on the In and N distribution in InGaAsN quantum wells, *Applied Physics Letters* 81: 2719–2721.
- Bastard, G. A. (1988). *Wave mechanics applied to semiconductor heterostructures*, Les Editions de Physique, Paris.
- Bastard, G. & Brum, J. (1986). Electronic states in semiconductor heterostructures, *Quantum Electronics, IEEE Journal of* 22: 1625–1644.
- Bhat, R., Caneau, C., Salamanca-Riba, L., Bi, W. & Tu, C. (1998). Growth of GaAsN/GaAs, GaInAsN/GaAs and GaInAsN/GaAs quantum wells by low-pressure organometallic chemical vapor deposition, *Journal of Crystal Growth* 195: 427–437.
- Buyanova, I. A., Chen, W. M., Pozina, G., Bergman, J. P., Monemar, B., Xin, H. P. & Tu, C. W. (1999). Mechanism for low-temperature photoluminescence in GaNAs/GaAs structures grown by molecular-beam epitaxy, *Applied Physics Letters* 75: 501–504.
- Buyanova, I. A., Chen, W. M. & Tu, C. W. (2002). Magneto-optical and light-emission properties of III-As-N semiconductors, *Semiconductor Science and Technology* 17: 815–822.
- Buyanova, I. A., Chen, W. M. & Tu, C. W. (2003). Recombination processes in N-containing III-V ternary alloys, *Solid State Electronics* 47: 467–475.
- Buyanova, I. A., Hai, P. N., Chen, W. M., Xin, H. P. & Tu, C. W. (2000). Direct determination of electron effective mass in GaNAs/GaAs quantum wells, *Applied Physics Letters* 77: 1843–1845.
- Buyanova, I. A., Pozina, G., Hai, P. N. & Chen, W. M. (2000). Type I band alignment in the GaN_xAs_{1-x}/GaAs quantum wells, *Physical Review B* 63: 033303–033307.
- Buyanova, I. A., Pozina, G., Hai, P. N., Thinh, N. Q., Bergman, J. P., Chen, W. M., Xin, H. P. & Tu, C. W. (2000). Mechanism for rapid thermal annealing improvements in undoped GaN(x)As(1-x)/GaAs structures grown by molecular beam epitaxy, *Applied Physics Letters* 77: 2325–2327.
- de Walle, C. G. V. (1989). Band lineups and deformation potentials in the model-solid theory, *Physical Review B* 39: 1871–1883.
- Egorov, A. Y., Odnobludov, V. A., Zhukov, A. E., Tsatsul'nikov, A. F., Krizhanovskaya, N. V., Ustinov, V. M., Hong, Y. G. & Tu, C. W. (2002). Valence band structure of GaAsN compounds and band-edge line-up in GaAs/GaAsN/InGaAs heterostructures, *Molecular Beam Epitaxy, 2002 International Conference on*, IEEE, pp. 269–270.
- Esaki, L. & Tsu, R. (1970). Superlattice and negative differential conductivity in semiconductors, *IBM J. Res. Development* 14: 61–65.
- Fan, W. J., Li, M. F., Chong, T. C. & Xia, J. B. (1996). Electronic properties of zinc-blende GaN, AlN, and their alloys Ga_{1-x}Al_xN, *Journal of Applied Physics* 79: 188–194.
- Francoeur, S., Sivaraman, G., Qiu, Y., Nikishin, S. & Temkin, H. (1998). Luminescence of as-grown and thermally annealed GaAsN/GaAs, *Applied Physics Letters* 72: 1857–1859.
- Geisz, J. F., Friedman, D. J., Olson, J. M., Kurtz, S. R. & Keyes, B. M. (1998). Photocurrent of 1 eV GaInNAs lattice-matched to GaAs, *Journal of Crystal Growth* 195: 401–408.
- Gerard, J. M., Marzin, J. Y., Jusserand, B., Glas, F. & Primot, J. (1989). Structural and optical properties of high quality InAs/GaAs short-period superlattices grown by migration-enhanced epitaxy, *Applied Physics Letters* 54: 30–32.

- Gilet, P., Chevenas-Paule, A., Duvaut, P., Grenouillet, L., Hollinger, P., Million, A., Rolland, G. & Vannuffel, C. (1999). Growth and characterization of thick GaAsN epilayers and GaInNAs/GaAs multiquantum wells, *Physica-Status-Solidi a* 176: 279–283.
- Grenouillet, L., Bru-Chevallier, C., Guillot, G., Gilet, P., Ballet, P., Duvaut, P., Rolland, G. & Million, A. (2002). Rapid thermal annealing in GaN_xAs_{1-x}/GaAs structures: Effect of nitrogen reorganization on optical properties, *Journal of Applied Physics* 91: 5902–5908.
- Gupta, J. A., Barrios, P. J., Aers, G. C., Williams, R. L., Ramsey, J. & Wasilewski, Z. R. (2003). Properties of 1.3 μm InGaNAs laser material grown by MBE using a N₂/Ar RF plasma, *Solid State Electronics* 47: 399–405.
- Hasenberg, T. C., McCallum, D. S., Huang, X. R., Dawson, M. D., Boggess, T. F. & Smirl, A. L. (1991). Linear optical properties of quantum wells composed of all-binary InAs/GaAs short-period strained-layer superlattices, *Applied Physics Letters* 58: 937–939.
- Hierro, A., Ulloa, J.-M., Chauveau, J.-M., Trampert, A., Pinault, M.-A., Tournié, E., Guzmán, A., Sánchez-Rojas, J. L. & Calleja, E. (2003). Annealing effects on the crystal structure of GaInNAs quantum wells with large In and N content grown by molecular beam epitaxy, *Journal of Applied Physics* 94: 2319–2324.
- Hong, Y. G., Egorov, A. Y. & Tu, C. W. (2002). Growth of GaInNAs quaternaries using a digital alloy technique, *Journal of Vacuum Science Technology B* 20: 1163–1166.
- Hong, Y. G. & Tu, C. W. (2002). Optical properties of GaAs/GaN_xAs_{1-x} quantum well structures grown by migration-enhanced epitaxy, *Journal of Crystal Growth* 242: 29–34.
- Hong, Y. G., Tu, C. W. & Ahrenkiel, R. K. (2001). Improving properties of GaInNAs with a short-period GaInAs/GaNAs superlattice, *Journal of Crystal Growth* 227: 536–540.
- hsiu Ho, I. & Stringfellow, G. B. (1997). Solubility of nitrogen in binary III-V systems, *Journal of Crystal Growth* 178: 1–7.
- Jalili, Y. S., Stavrinou, P. N., Jones, T. & Parry, G. (2004). GaAs-based III-N_y-V_{1-y} active regions based on short-period super-lattice structures, to be submitted to, *Physical Review B*.
- Jang, J. G., Miller, D. L., Fu, J. & Zhang, K. (1992). Study of (InAs)_m(GaAs)_n short-period superlattice layers grown on GaAs substrates by molecular-beam epitaxy, *Journal of Vacuum Science Technology B* 10: 772–774.
- Kageyama, T., Miyamoto, T., Makino, S., Koyama, F. & Iga, K. (1999). Thermal annealing of GaInNAs/GaAs quantum wells grown by chemical beam epitaxy and its effect on photoluminescence, *Japanese Journal of Applied Physics* 38: L298–L300.
- Kent, P. R. C. & Zunger, A. (2001a). Evolution of III-V Nitride alloy electronic structure: The localized to delocalized transition, *Physical Review Letters* 86: 2613–2616.
- Kent, P. R. C. & Zunger, A. (2001b). Theory of electronic structure evolution in GaAsN and GaPN alloys, *Physical Review B* 64: 115208–115231.
- Kim, K., Lambrecht, W. R. L. & Segall, B. (1996). Elastic constants and related properties of tetrahedrally bonded BN, AlN, GaN, and InN, *Physical Review B* 53: 16310–16326.
- Kitatani, T., Kondow, M., Nakahara, K., Larson, M. C., Yazawa, Y., Okai, M. & Uomi, K. (1999). Nitrogen incorporation rate, optimal growth temperature, and AsH₃-flow rate in GaInNAs growth by gas-source MBE using N-radicals as an N-source, *Journal of Crystal Growth* 201-202: 351–354.
- Kitatani, T., Nakahara, K., Kondow, M., Uomi, K. & Tanaka, T. (2000). Mechanism analysis of improved GaInNAs optical properties through thermal annealing, *Journal of Crystal Growth* 209: 345–349.

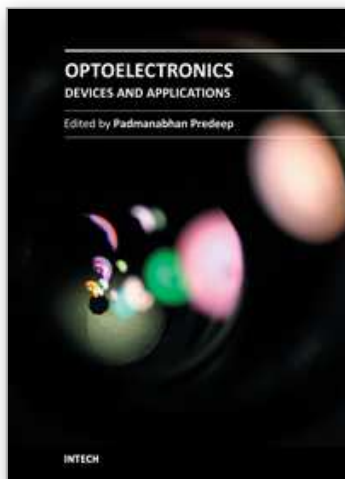
- Klar, P. J., Gruning, H., Chen, L., Hartmann, T., Golde, D., Gungerich, M., Heimbrodt, W., Koch, J., Volz, K., Kunert, B., Torunski, T., Stolz, W., Polimeni, A., Capizzi, M., Dumitras, G., Geelhaar, L. & Riechert, H. (2003). Unusual properties of metastable (Ga, In)(N,As) containing semiconductor structures, *in* IEEE (ed.), *Optoelectronics, IEE Proceedings-*, Vol. 150, IEEE, pp. 28–35.
- Klar, P. J., Gruning, H., Heimbrodt, W., Weiser, G., Koch, J., Volz, K., Stolz, W., Koch, S. W., Tomic, S., Choulis, S. A., Hosea, T. J. C., O'Reilly, E. P., Hofmann, M., Hader, J. & Moloney, J. V. (2002). Interband transitions of quantum wells and device structures containing Ga(N, As) and (Ga, In)(N, As), *Semiconductor Science and Technology* 17: 830–842.
- Klar, P. J., Gruning, H., Koch, J., Schafer, S., Volz, K., Stolz, W., Heimbrodt, W., Saadi, A. M. K., Lindsay, A. & O'SReilly, E. P. (2001). (Ga, In)(N, As)-fine structure of the band gap due to nearest-neighbor configurations of the isovalent nitrogen, *Physical Review B* 64: 121203(R)–121207(R).
- Kondow, M., Uomi, K., Kitatani, T., Watahiki, S. & Yazawa, Y. (1996). Extremely large N-content (up to 10%) in ganas grown by gas-source MBE, *Journal of Crystal Growth* 164: 175–179.
- Kong, J. A. (1990). *Electromagnetic wave theory*, 2nd edn, Wiley, New York.
- Kurtz, S., Webb, J., Gedvilas, L., Friedman, D., Geisz, J., Olson, J., King, R., Joslin, D. & Karam, N. (2001). Structural changes during annealing of GaInAsN, *Applied Physics Letters* 78: 748–750.
- Li, L. H., Pan, Z., Zhang, W., Lin, Y. W., Zhou, Z. Q. & Wu, R. H. (2000). Effects of rapid thermal annealing on the optical properties of GaN_xAs_{1-x}/GaAs single quantum well structure grown by molecular beam epitaxy, *Journal of Applied Physics* 87: 245–248.
- Li, W., Pessa, M., Ahlgren, T. & Decker, J. (2001). Origin of improved luminescence efficiency after annealing of Ga(In)NAs materials grown by molecular-beam epitaxy, *Applied Physics Letters* 79: 1094–1096.
- Li, W., Pessa, M. & Likonen, J. (2001). Lattice parameter in GaNAs epilayers on GaAs: Deviation from Vegard's law, *Applied Physics Letters* 78: 2864–2866.
- Lindsay, A. (2002). PhD Thesis, University of Surrey.
- Loke, W. K., Yoon, S. F., Wang, S. Z., Ng, T. K. & Fan, W. J. (2002). Rapid thermal annealing of GaN_xAs_{1-x} grown by radio-frequency plasma assisted molecular beam epitaxy and its effect on photoluminescence, *Journal of Applied Physics* 91: 4900–4903.
- Mair, R. A., Lin, J. Y., Jianga, H. X., Jones, E. D., Allerman, A. A. & Kurtz, S. R. (2000). Time-resolved photoluminescence studies of In(x)Ga(1-x)As(1-y)N(y), *Applied Physics Letters* 76: 188–190.
- Masia, F., Polimeni, A., Baldassarri, G., von Högersthal, H., Bissiri, M., Capizzi, M., Klar, P. J. & Stolz, W. (2003). Early manifestation of localization effects in diluted Ga(AsN), *Applied Physics Letters* 82: 4474–4476.
- Mazzucato, S., Potter, R. J., Erol, A., Balkan, N., Chalker, P. R., Joyce, T. B., Bullough, T. J., Marie, X., Carrère, H., Bedel, E., Lacoste, G., Arnoult, A. & Fontaine, C. (2003). S-shaped behaviour of the temperature-dependent band gap in dilute nitrides, *Physica E* 17: 242–244.
- Miyamoto, T., Kageyama, T., Makino, S., Schlenker, D., Koyama, F. & Iga, K. (2000). CBE and MOCVD growth of GaInNAs, *Journal of Crystal Growth* 209: 339–344.

- Moison, J. M., Guille, C., Houzay, F., Barthe, F. & Rompay, M. V. (1989). Surface segregation of third-column atoms in group iii-v arsenide compounds: ternary alloys and heterostructures, *Physical Review B* 40: 6149–6162.
- Moreira, M. V. B., Py, M. A. & Ilegems, M. (1993). Molecular-beam epitaxial growth and characterization of modulation-doped field-effect transistor heterostructures using InAs/GaAs superlattice channels, *Journal of Vacuum Science Technology B* 11: 601–609.
- Mussler, G., Däweritz, L., K H Ploog, J. W. T. & Talalaev, V. (2003). Optimized annealing conditions identified by analysis of radiative recombination in dilute Ga(As,N), *Applied Physics Letters* 83: 1343–1345.
- Ng, T. K., Yoon, S. F., Wang, S. Z., Loke, W. K. & Fan, W. J. (2002). Photoluminescence characteristics of GaInNAs quantum wells annealed at high temperature, *Journal of Vacuum Science Technology B* 20: 964–968.
- O'Reilly, E. P., Lindsay, A., Tomic, S. & Kamal-Saadi, M. (2002). Tight-binding and $\mathbf{k}\cdot\mathbf{p}$ models for the electronic structure of Ga(In)NAs and related alloys, *Semiconductor Science and Technology* 17: 870–879.
- Ougazazaden, A., Bellego, Y. L., Rao, E. V. K., Juhel, M. & Leprince, L. L. (1997). Metal organic vapor phase epitaxy growth of GaAsN on GaAs using dimethylhydrazine and tertiarybutylarsine, *Applied Physics Letters* 70: 2861–2863.
- Pan, Z., Li, L. H., Zhang, W., Lin, Y. W. & Wu, R. H. (2000). Effect of rapid thermal annealing on GaInNAs/GaAs quantum wells grown by plasma-assisted molecular-beam epitaxy, *Applied Physics Letters* 77: 1280–1282.
- Pearton, S. J. (2000). *Optoelectronic properties of semiconductors and superlattices: GaN and related materials II*, Gordon and Breach Science Publishers.
- Peng, C. S., Pavelescu, E. M., Jouhti, T., Konttinen, J. & Pessa, M. (2003). Diffusion at the interfaces of InGaNAs/GaAs quantum wells, *Solid State Electronics* 47: 431–435.
- Persson, C., da Silva, A. F., Ahuja, R. & Johansson, B. (2001). Effective electronic masses in wurtzite and zinc-blende GaN and AlN, *Journal of Crystal Growth* 231: 397–406.
- Polimeni, A., v H G Baldassarri, H., Bissiri, M., Capizzi, M., Fischer, M., Reinhardt, M. & Forchel, A. (2001). Effect of hydrogen on the electronic properties of $\text{In}_x\text{Ga}_{1-x}\text{As}_{1-y}\text{N}_y/\text{GaAs}$ quantum wells, *Physical Review B* 63: 201304(R)–201308(R).
- Pomarico, A., Lomascolo, M., Cingolani, R., Egorov, A. Y. & Riechert, H. (2002). Effects of thermal annealing on the optical properties of InGaNAs/GaAs multiple quantum wells, *Semiconductor Science and Technology* 17: 145–149.
- Raja, M., Lloyd, G. C. R., Sedghi, N., Eccleston, W., Lucrezia, R. D. & Higgins, S. J. (2002). Conduction processes in conjugated, highly regio-regular, high molecular mass, poly(3-hexylthiophene) thin-film transistors, *Journal of Applied Physics* 92: 1446–1449.
- Ram-Mohan, L. R., Yoo, K. H. & Aggarwal, R. L. (1988). Transfer matrix algorithm for the calculation of band structure of semiconductor super lattices, *Physical Review B* 38: 6151–6159.
- Rao, E. V. K., Ougazzaden, A., Begello, Y. L. & Juhel, M. (1998). Optical properties of low band gap $\text{GaAs}_{1-x}\text{N}_x$ layers: Influence of post-growth treatments, *Applied Physics Letters* 72: 1409–1411.
- Sai-Halasz, G. A., Tsu, R. & Esaki, L. (1977). A new semiconductor superlattice, *Applied Physics Letters* 30: 651–653.
- Saito, H., Makimoto, T. & Kobayashi, N. (1998). MOVPE growth of strained InGaAsN/GaAs quantum wells, *Journal of Crystal Growth* 195: 416–420.

- Seong, M. J., Hanna, M. C. & Mascarenhas, A. (2001). Composition dependence of Raman intensity of the nitrogen localized vibrational mode in GaAs(1-x)N(x), *Applied Physics Letters* 79: 3974–3976.
- Shan, W., Walukiewicz, W., III, J. W. A., Haller, E. E., Geisz, J. F., Friedman, D. J., Olson, J. M. & Kurtz, S. R. (1999). Band anticrossing in GaInNAs alloys, *Physical Review Letters* 82: 1221–1224.
- Shan, W., Walukiewicz, W., Yu, K. M., III, J. W. A., Haller, E. E., Geisz, J. F., Friedman, D. J., Olson, J. M., Kurtz, S. R., Xin, H. P. & Tu, C. (2001). Band anticrossing in III-N-V alloys, *Physica-Status-Solidi B* 223: 75–85.
- Shirakata, S., Kondow, M. & Kitatani, T. (2002). Temperature-dependent photoluminescence of high-quality GaInNAs single quantum wells, *Applied Physics Letters* 80: 2087–2089.
- Sik, J., Schubert, M., Leibiger, G., Gottschalch, V. & Wagner, G. (2001). Band-gap energies, free carrier effects, and phonon modes in strained GaNAs/GaAs and GaNAs/InAs/GaAs superlattice heterostructures measured by spectroscopic ellipsometry, *Journal of Applied Physics* 89: 294–305.
- Skierbiszewski, C., Perlin, P., Wisniewski, P., Knapp, W., Suski, T., Walukiewicz, W., Shan, W., Yu, K. M., Ager, J. W., Haller, E. E., Geisz, J. F. & Olson, J. M. (2000). Large, nitrogen-induced increase of the electron effective mass in $\text{In}_y\text{Ga}_{1-y}\text{N}_x\text{As}_{1-x}$, *Applied Physics Letters* 76: 2409–2411.
- Spruytte, S. G., Coldren, C. W., Harris, J. S., Wampler, W., Krispin, P., Ploog, K. & Larson, M. C. (2001a). Incorporation of nitrogen in nitride-arsenides: Origin of improved luminescence efficiency after anneal, *Journal of Applied Physics* 89: 4401–4406.
- Spruytte, S. G., Coldren, C. W., Harris, S. J., Wampler, W., Krispin, P., Ploog, K. & Larson, M. C. (2001b). Incorporation of nitrogen in nitride-arsenides: Origin of improved luminescence efficiency after anneal, *Journal of Applied Physics* 89: 4401–4406.
- Toivonen, J., Hakkarainen, T., Sopanen, M. & Lipsanen, H. (2003a). Effect of post-growth laser treatment on optical properties of Ga(In)NAs quantum wells, in *IEEE (ed.), Optoelectronics, IEE Proceedings-*, Vol. 150, IEE, pp. 68–71.
- Toivonen, J., Hakkarainen, T., Sopanen, M. & Lipsanen, H. (2003b). Observation of defect complexes containing Ga vacancies in GaAsN, *Applied Physics Letters* 82: 40–42.
- Tournie, E., Pinault, M.-A. & Guzman, A. (2002). Mechanisms affecting the photoluminescence spectra of GaInNAs after post-growth annealing, *Applied Physics Letters* 80: 4148–4150.
- Toyoshima, H., Anan, T., Nishi, K., Ichihashi, T. & Okamoto, A. (1990). Growth by molecular-beam epitaxy and characterization of $(\text{InAs})_m(\text{GaAs})_n$ short period superlattices on InP substrates, *Journal of Applied Physics* 68: 1282–1286.
- Toyoshima, H., Onda, K., Mizuki, E., Samoto, N., Kuzuhara, M., Itoh, T., Okamoto, A., Anan, T. & Ichihashi, T. (1991). Molecular-beam epitaxial growth of InAs/GaAs superlattices on GaAs substrates and its application to a superlattice channel modulation-doped field-effect transistor, *Journal of Applied Physics* 69: 3941–3949.
- v H G Baldassarri, H., Bissiri, M., Polimeni, A., Capizzi, M., Fischer, M., Reinhardt, M. & Forchel, A. (2001). Hydrogen-induced band gap tuning of (InGa)(AsN)/GaAs single quantum wells, *Applied Physics Letters* 78: 3472–3474.
- Wagner, J., Geppert, T., Köhler, K., Ganser, P. & Maier, M. (2003). Bonding of nitrogen in dilute GaInAsN and AlGaAsN studied by raman spectroscopy, *Solid State Electronics* 47: 461–465.

- Wang, S. Z., Yoon, S. F., Loke, W. K., Liu, C. Y. & Yuan, S. (2003). Origin of photoluminescence of GaAsN/GaN(001) layers grown by plasma-assisted solid source molecular beam epitaxy, *Journal of Crystal Growth* 255: 258–265.
- Wang, S. Z., Yoon, S. F., Ng, T. K., Loke, W. K. & Fan, W. J. (2002). Molecular beam epitaxial growth of GaAs_{1-x}N_x with dispersive nitrogen source, *Journal of Crystal Growth* 242: 87–94.
- Weyers, M., Sato, M. & Ando, H. (1992). Red shift of photoluminescence and absorption in dilute GaAsN alloy lasers, *Japanese Journal of Applied Physics* 31: L853–L857.
- Xin, H. P., Kavanagh, K. L. & Tu, C. W. (2000). Gas-source molecular beam epitaxial growth and thermal annealing of GaInNAs/GaAs quantum wells, *Journal of Crystal Growth* 208: 145–152.
- Xin, H. P., Tu, C. W. & Geva, M. (1999). Annealing behaviour of p-type GaInAsN grown by GSMBE, *Applied Physics Letters* 75: 1416–1418.
- Yeh, P. & Yariv, A. (1984). *Optical waves in crystals*, John Wiley and Sons, New York.

IntechOpen



Optoelectronics - Devices and Applications

Edited by Prof. P. Predeep

ISBN 978-953-307-576-1

Hard cover, 630 pages

Publisher InTech

Published online 03, October, 2011

Published in print edition October, 2011

Optoelectronics - Devices and Applications is the second part of an edited anthology on the multifaced areas of optoelectronics by a selected group of authors including promising novices to experts in the field. Photonics and optoelectronics are making an impact multiple times as the semiconductor revolution made on the quality of our life. In telecommunication, entertainment devices, computational techniques, clean energy harvesting, medical instrumentation, materials and device characterization and scores of other areas of R&D the science of optics and electronics get coupled by fine technology advances to make incredibly large strides. The technology of light has advanced to a stage where disciplines sans boundaries are finding it indispensable. New design concepts are fast emerging and being tested and applications developed in an unimaginable pace and speed. The wide spectrum of topics related to optoelectronics and photonics presented here is sure to make this collection of essays extremely useful to students and other stake holders in the field such as researchers and device designers.

How to reference

In order to correctly reference this scholarly work, feel free to copy and paste the following:

Y Seyed Jalili (2011). SPSLs and Dilute-Nitride Optoelectronic Devices, Optoelectronics - Devices and Applications, Prof. P. Predeep (Ed.), ISBN: 978-953-307-576-1, InTech, Available from: <http://www.intechopen.com/books/optoelectronics-devices-and-applications/spsls-and-dilute-nitride-optoelectronic-devices>

INTECH
open science | open minds

InTech Europe

University Campus STeP Ri
Slavka Krautzeka 83/A
51000 Rijeka, Croatia
Phone: +385 (51) 770 447
Fax: +385 (51) 686 166
www.intechopen.com

InTech China

Unit 405, Office Block, Hotel Equatorial Shanghai
No.65, Yan An Road (West), Shanghai, 200040, China
中国上海市延安西路65号上海国际贵都大饭店办公楼405单元
Phone: +86-21-62489820
Fax: +86-21-62489821

© 2011 The Author(s). Licensee IntechOpen. This is an open access article distributed under the terms of the [Creative Commons Attribution 3.0 License](#), which permits unrestricted use, distribution, and reproduction in any medium, provided the original work is properly cited.

IntechOpen

IntechOpen